nature biotechnology

ARTICLES

https://doi.org/10.1038/s41587-020-00796-1

Hypertension delays viral clearance and exacerbates airway hyperinflammation in patients with COVID-19

Saskia Trump[1,17], Soeren Lukassen[2,17], Markus S. Anker[3,4,5,6,17], Robert Lorenz Chua[2,17], Johannes Liebig[2,17], Loreen Thürmann[1,17], Victor Max Corman[7,17], Marco Binder[8,17], Jennifer Loske[1], Christina Klasa[9], Teresa Krieger[2], Bianca P. Hennig[2], Marey Messingschlager[1], Fabian Pott[7,10], Julia Kazmierski[7,10], Sven Twardziok[2], Jan Philipp Albrecht[2], Jürgen Eils[2], Sara Hadzibegovic[3,4,5,6], Alessia Lena[3,4,5,6], Bettina Heidecker[3], Thore Bürgel[2], Jakob Steinfeldt[3], Christine Goffinet[7,10], Florian Kurth[11,12], Martin Witzenrath[11], Maria Theresa Völker[13], Sarah Dorothea Müller[13], Uwe Gerd Liebert[14], Naveed Ishaque[2], Lars Kaderali[9], Leif-Erik Sander[11], Christian Drosten[7], Sven Laudi[13,18] ✉, Roland Eils[2,15,16,18] ✉, Christian Conrad[2,18] ✉, Ulf Landmesser[3,18] ✉ and Irina Lehmann[1,15,18] ✉

In coronavirus disease 2019 (COVID-19), hypertension and cardiovascular diseases are major risk factors for critical disease progression. However, the underlying causes and the effects of the main anti-hypertensive therapies—angiotensin-converting enzyme inhibitors (ACEIs) and angiotensin receptor blockers (ARBs)—remain unclear. Combining clinical data ($n = 144$) and single-cell sequencing data of airway samples ($n = 48$) with in vitro experiments, we observed a distinct inflammatory predisposition of immune cells in patients with hypertension that correlated with critical COVID-19 progression. ACEI treatment was associated with dampened COVID-19-related hyperinflammation and with increased cell intrinsic antiviral responses, whereas ARB treatment related to enhanced epithelial–immune cell interactions. Macrophages and neutrophils of patients with hypertension, in particular under ARB treatment, exhibited higher expression of the pro-inflammatory cytokines *CCL3* and *CCL4* and the chemokine receptor *CCR1*. Although the limited size of our cohort does not allow us to establish clinical efficacy, our data suggest that the clinical benefits of ACEI treatment in patients with COVID-19 who have hypertension warrant further investigation.

Of patients hospitalized for COVID-19, males and those of older age have a higher risk for critical disease[1,2]. Hypertension, which is highly prevalent in adults worldwide[3], has been identified as a major risk factor for increased COVID-19 severity[4,5]. Hypertensive patients with COVID-19 are more likely to develop severe pneumonia or organ damage than patients without hypertension. In addition, these patients exhibit exacerbated inflammatory responses and have a higher risk of dying from COVID-19 than patients without hypertension[4,6].

Severe acute respiratory syndrome coronavirus 2 (SARS-CoV-2), the virus that causes COVID-19, exploits the ACE2 receptor, expressed on epithelial cells in the respiratory system, for cellular

[1]Molecular Epidemiology Unit, Charité - Universitätsmedizin Berlin, corporate member of Freie Universität Berlin, Humboldt-Universität zu Berlin, and Berlin Institute of Health (BIH), Berlin, Germany. [2]Center for Digital Health, Berlin Institute of Health (BIH) and Charité - Universitätsmedizin Berlin, corporate member of Freie Universität Berlin, Humboldt-Universität zu Berlin, Berlin, Germany. [3]Department of Cardiology, Campus Benjamin Franklin, Charité - Universitätsmedizin Berlin, corporate member of Freie Universität Berlin, Humboldt-Universität zu Berlin, and Berlin Institute of Health (BIH), Berlin, Germany. [4]Division of Cardiology and Metabolism, Department of Cardiology Campus Virchow, Charité - Universitätsmedizin Berlin, corporate member of Freie Universität Berlin, Humboldt-Universität zu Berlin, and Berlin Institute of Health (BIH), Berlin, Germany. [5]Centre for Cardiovascular Research (DZHK), Berlin, Germany. [6]Berlin Institute of Health Center for Regenerative Therapies (BCRT), Berlin, Germany. [7]Institute of Virology, Charité - Universitätsmedizin Berlin, corporate member of Freie Universität Berlin, Humboldt-Universität zu Berlin, and Berlin Institute of Health (BIH), Berlin, Germany. [8]Research group 'Dynamics of early viral infection and the innate antiviral response' (division F170), German Cancer Research Center (DKFZ), Heidelberg, Germany. [9]Institute for Bioinformatics, University Medicine Greifswald, Greifswald, Germany. [10]Berlin Institute of Health (BIH), Berlin, Germany. [11]Department of Infectious Diseases and Respiratory Medicine, Charité - Universitätsmedizin Berlin, corporate member of Freie Universität Berlin, Humboldt-Universität zu Berlin, and Berlin Institute of Health (BIH), Berlin, Germany. [12]Department of Tropical Medicine, Bernhard Nocht Institute for Tropical Medicine & I. Department of Medicine, University Medical Center Hamburg-Eppendorf, Hamburg, Germany. [13]Department of Anesthesiology and Intensive Care, University Hospital Leipzig, Leipzig, Germany. [14]Institute of Virology, University Hospital Leipzig, Leipzig, Germany. [15]German Center for Lung Research (DZL), Berlin, Germany. [16]Health Data Science Unit, Medical Faculty and BioQuant, University of Heidelberg, Heidelberg, Germany. [17]These authors contributed equally: Saskia Trump, Soeren Lukassen, Markus S. Anker, Robert Lorenz Chua, Johannes Liebig, Loreen Thürmann, Victor Max Corman, Marco Binder. [18]These authors jointly supervised this work: Sven Laudi, Roland Eils, Christian Conrad, Ulf Landmesser, Irina Lehmann. ✉e-mail: sven.laudi@medizin.uni-leipzig.de; roland.eils@charite.de; christian.conrad@charite.de; ulf.landmesser@charite.de; irina.lehmann@charite.de

attachment and entry[7]. ACE2 is a membrane-bound aminopeptidase and is part of the non-canonical arm of the renin–angiotensin–aldosterone system (RAAS), which regulates blood pressure homeostasis and vascular repair responses. It has been speculated that anti-hypertensive treatment by ACEIs or ARBs might modulate ACE2 expression and, thereby, alter susceptibility for SARS-CoV-2 infection. In the classical RAAS pathway, angiotensin II binds to the angiotensin II receptor subtype 1 (AT1R), which promotes vasoconstriction and pro-inflammation. ACE2, on the other hand, cleaves angiotensin II into angiotensin 1–7 and angiotensin I into angiotensin 1–9, both mediating vasodilatatory and anti-inflammatory effects[8,9]. Several different compounds of ACEI (for example, ramipril and enalapril) and ARB (for example, candesartan and valsartan) are used in clinical practice, which have a similar mode of action within their class[10].

Data from animal studies demonstrated that ACEIs and ARBs can upregulate *ACE2* expression[11], raising the question of whether an increase in the availability of SARS-CoV-2 receptors in patients treated with ACEIs or ARBs[12,13] rendered them more susceptible to viral infection and spread. To date, there is no evidence from observational studies that ACEI or ARB treatment could increase the infectivity for SARS-CoV-2 (refs. [4,14]).

Hypertension is associated with the activation of inflammatory processes[15–19]. As a hyperinflammatory phenotype in the respiratory system has been described to enhance the severity of COVID-19 (refs. [20,21]), we assessed whether a potential pro-inflammatory predisposition of patients with hypertension before SARS-CoV-2 infection might contribute to an exacerbated disease severity.

To this end, we evaluated the effect of coexisting cardiovascular illnesses, in particular of hypertension and anti-hypertensive treatment, on COVID-19 pathology and viral clearance based on two German prospective cohorts. By analyzing the single-cell transcriptome landscape of the airways of patients with COVID-19 and SARS-CoV-2$^-$ controls, we provide insights into the differential COVID-19 pathology in patients treated with ACEI/ARB compared to patients without cardiovascular diseases or with a different anti-hypertensive treatment.

Results

ACEI/ARB treatment was associated with a lower hypertension-related risk for critical COVID-19. We first assessed the effect of hypertension (HT$^+$) and other cardiovascular diseases (CVD$^+$) with anti-hypertensive treatment on COVID-19 severity (Fig. 1a). Both medical conditions have been associated with an adverse outcome in COVID-19 (refs. [4,12–14,22–24]). Accordingly, we compared the proportion of critical cases to all other severities of COVID-19 in the different patient groups of the Pa-COVID-19 cohort[25] (see Supplementary Table 1 for clinical characteristics). The proportion of patients with a critical outcome was significantly increased for HT$^+$/CVD$^{+/-}$ patients ($n=90$) compared to HT$^-$/CVD$^-$ patients with COVID-19 ($n=54$, $P = 0.002$). For HT$^+$ patients, the proportion for critical COVID-19 was highest without ACEI or ARB treatment: almost 77% of HT$^+$/CVD$^-$ patients without ACEI or ARB and over 70% of HT$^+$/CVD$^+$ patients without ACEI or ARB showed critical COVID-19 (Supplementary Table 2 and Fig. 1a). In contrast, ACEI and ARB treatments were associated with a decreased proportion of critical COVID-19 in both groups (HT$^+$/CVD$^-$ and HT$^+$/CVD$^+$); however, ACEI treatment showed a more profound decline in critical cases as compared to ARB treatment. ACEI-treated HT$^+$/CVD$^{+/-}$ patients showed almost the same proportion of critical COVID-19 as HT$^-$/CVD$^-$ patients (Supplementary Table 2 and Fig. 1a).

To exclude the effect of other risk factors for an adverse COVID-19 clinical course, we performed logistic regression analyses adjusted for known confounding factors, including age, sex, body mass index (BMI) and co-treatment with other commonly used cardiovascular therapeutics, such as statins and beta blockers. This analysis confirmed a higher risk for developing critical COVID-19 for hypertensive patients with/without a coexisting cardiovascular disease (HT$^+$/CVD$^{+/-}$) over non-hypertensive patients (HT$^-$/CVD$^-$; adjusted odds ratio (adjOR) = 4.28, 95% confidence interval (CI): 1.60–11.46, $P = 0.028$; Fig. 1a, upper panel). The logistic regression analysis revealed no significant increase for critical COVID-19 in hypertensive patients with ACEI treatment compared to non-hypertensive patients (HT$^+$/CVD$^-$/ACEI$^+$ versus HT$^-$/CVD$^-$; Fig. 1a, middle panel). In contrast, patients treated with ARB still had an increased risk for critical COVID-19 compared to non-hypertensive patients (HT$^-$/CVD$^-$ versus HT$^+$/CVD$^-$/ARB$^+$) (adjOR = 4.14, 95% CI: 1.01–17.04, $P = 0.044$; Fig. 1a, middle panel). However, this risk for critical disease was lower than for hypertensive patients without ACEI or ARB treatment (HT$^-$/CVD$^-$ versus HT$^+$/CVD$^-$/ACEI$^-$/ARB$^-$: adjOR = 8.17, 95% CI:1.65–40.52, $P = 0.009$; Fig. 1a). In trend, similar results were observed for HT$^+$/CVD$^+$ patients (Fig. 1a, lower panel) without reaching the significance level, likely owing to lower case numbers.

Our results showed that patients with hypertensive disease had an increased risk for critical COVID-19. This risk was lower in ACEI/ARB-treated patients. ACEI treatment almost entirely abolished the additional risk related to hypertension, whereas ARB treatment was associated with only a reduced risk.

ARB but not ACEI treatment was associated with delayed SARS-CoV-2 clearance. We investigated the dynamics of SARS-CoV-2 clearance in patients included in the Pa-COVID-19 cohort. During hospitalization, patients with COVID-19 were tested longitudinally for SARS-CoV-2 by quantitative polymerse chain reaction (qPCR) of the viral genome. Using an adjusted repeated measurement mixed model, we studied the changes of the viral load over time, comparing ACEI$^+$ ($n=21$) or ARB$^+$ ($n=26$) patients with COVID-19 to HT$^-$/CVD$^-$ patients with COVID-19 ($n=46$). All three groups showed the same initial viral load. Although ACEI$^+$ treatment did not change viral clearance up to 16 d after the first positive test compared to HT$^-$/CVD$^-$, ARB treatment was associated with a significantly slower viral clearance over time compared to HT$^-$/CVD$^-$ ($P = 0.031$) or ACEI$^+$ ($P = 0.026$) (Fig. 1b), respectively. This finding was supported by the time-dependent slope of viral load between the different patient groups. ARB$^+$ patients tended to have a flatter slope compared to HT$^-$/CVD$^-$ ($P = 0.07$; Extended Data Fig. 1a). The same was observed for HT$^+$/CVD$^{+/-}$ patients who showed a tendency of slower viral clearance compared to HT$^-$/CVD$^-$ patients ($P = 0.08$; Extended Data Fig. 1b).

Taken together, we showed that viral clearance in HT$^+$/CVD$^{+/-}$ patients under ACEI treatment was similar to that in patients with COVID-19 without a coexisting cardiovascular disease, whereas viral clearance might have been delayed in patients undergoing hypertensive ARB treatment.

Cardiovascular disease and SARS-CoV-2 infection affect cell type distribution. To investigate the cellular and molecular effect of cardiovascular comorbidities and anti-hypertensive treatment on COVID-19 severity, we performed extensive single-cell transcriptome profiling of nasopharyngeal samples from patients with COVID-19 with or without hypertension and other cardiovascular diseases (see Supplementary Table 3 for clinical characteristics). To disentangle the effect of HT and CVD on SARS-CoV-2 infection, we also included a mirror cohort of patients negative for SARS-CoV-2 with and without HT/CVD under ARB/ACEI treatment (Fig. 2a). In total, we assessed the transcriptomes of 114,761 individual cells obtained from nasopharyngeal swabs of 32 patients with COVID-19 ($n=25$ with HT$^+$/CVD$^{+/-}$; $n=10$ ACEI$^+$ and $n=15$ ARB$^+$; for treatment, see Supplementary Table 3) and 16

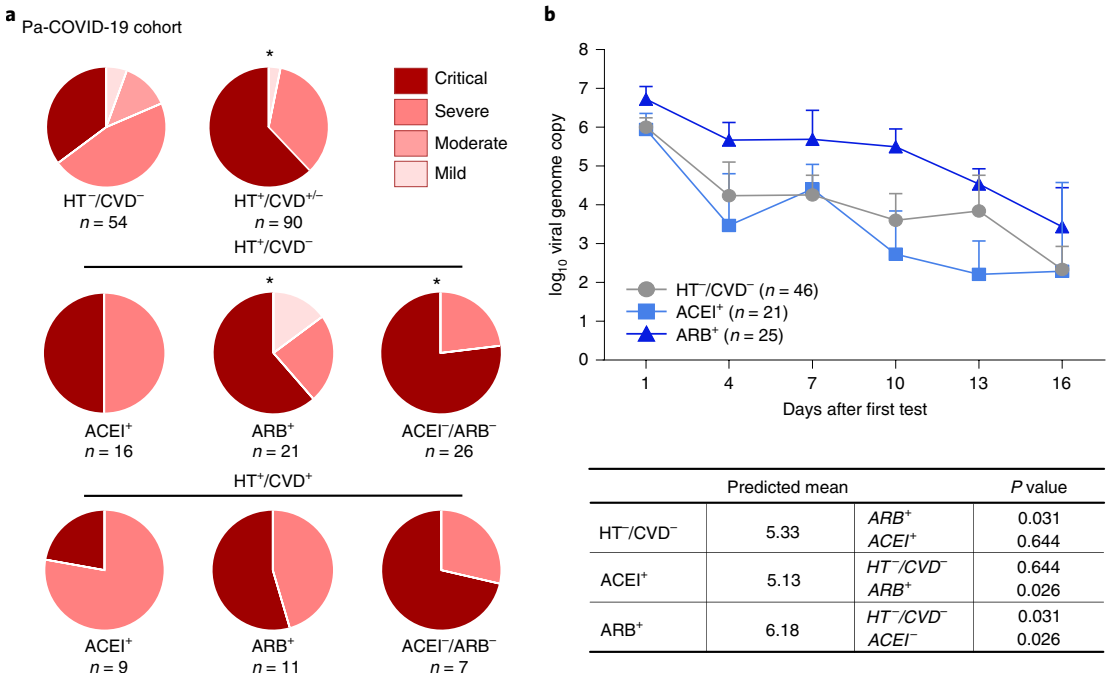

	Predicted mean		P value
HT⁻/CVD⁻	5.33	*ARB⁺*	0.031
		ACEI⁺	0.644
ACEI⁺	5.13	*HT⁻/CVD⁻*	0.644
		ARB⁺	0.026
ARB⁺	6.18	*HT⁻/CVD⁻*	0.031
		ACEI⁻	0.026

Fig. 1 | Association of anti-hypertensive treatment with COVID-19 severity and viral clearance in the Pa-COVID-19 cohort. a, Comparison of COVID-19 severity based on WHO classification in patients without cardiovascular comorbidities (HT⁻/CVD⁻, $n=54$) and those with arterial hypertension or cardiovascular disease (HT⁺/CVD⁺/⁻, $n=90$). Patients were separated into those with HT only (HT⁺/CVD⁻, $n=63$) and those with additional cardiovascular diseases (HT⁺/CVD⁺, $n=27$) and are depicted dependent on their treatment with ARB (ARB⁺), ACEI (ACEI⁺) or other medications (ACEI⁻/ARB⁻). $P<0.05$ based on chi-square tests comparing the number of critical patients versus patients with COVID-19 of all other WHO categories. All comparisons were made against the HT⁻/CVD⁻ group; for exact P values, refer to Supplementary Table 2. **b**, Viral clearance over time shown for patients positive for SARS-CoV-2 without a coexisting cardiovascular disease (CVD⁻/HT⁻, $n=46$) in comparison to ARB⁺ ($n=25$) or ACEI⁺ ($n=21$) HT⁺/CVD⁺/⁻ patients with COVID-19. Depicted are mean ± s.d. of qPCR data binned in 3-d intervals; only the maximal value of each patient in this interval was considered. Adjusted regression analysis (confounder: BMI, gender, smoking, insulin treatment and days after onset of symptoms; $n=92$) showed a significantly higher viral load for ARB⁺ HT⁺/CVD⁺/⁻ compared to ACEI⁺ HT⁺/CVD⁺/⁻ and HT⁻/CVD⁻ patients. Predicted means were calculated using maximum likelihood, and P values were derived from Fisher's LSD.

SARS-CoV-2⁻ controls ($n=10$ with HT⁺/CVD⁺/⁻; $n=6$ ACEI⁺ and $n=4$ ARB⁺; for treatment, see Supplementary Table 3). There was no significant difference in systolic or diastolic blood pressure between the ACEI- and ARB-treated patients at the day of sampling (systolic: 130.6 ± 16.3 mmHg versus 130.4 ± 14.2 mmHg, $P = 0.97$; diastolic: 74.7 ± 9.7 mmHg versus 69.7 ± 14.7 mmHg, $P = 0.26$). There was also no difference when comparing HT⁻/CVD⁻ patients (systolic: 118.9 ± 17.0 mmHg; diastolic: 67.7 ± 10.3 mmHg) to those treated with ACEIs or ARBs (systolic: $P = 0.21$; diastolic: $P = 0.36$). Only individuals diagnosed with severe to critical COVID-19 or SARS-CoV-2⁻ controls were eligible for inclusion in this part of the study (Supplementary Table 3).

We identified nine immune and 12 epithelial cell populations (Fig. 2b,c and Extended Data Fig. 2). Overall, SARS-CoV-2 infection led to pronounced changes in most epithelial and immune cells and cell states (Fig. 2c and Extended Data Fig. 3). In HT⁺/CVD⁺/⁻ patients with COVID-19, secretory and ciliated cells, known to be primarily infected by the virus[20,26–28], tended to be significantly decreased compared to HT⁻/CVD⁻ patients. This was accompanied by an expansion of non-resident macrophages (nrMa) and monocyte-derived macrophages (moMa), independent of their anti-hypertensive treatment (Fig. 2c and Extended Data Fig. 3).

Anti-hypertensive treatment is not associated with altered expression of the SARS-CoV-2 entry receptor *ACE2*. SARS-CoV-2 enters the human cell via the receptor ACE2 and with the help of the protease TMPRSS2. It has been speculated that ARB and ACEI, as RAAS-modulating agents, might change *ACE2* expression and, thereby, the infectivity for SARS-CoV-2. Because the expression of *ACE2* is generally low in human airways[26], we quantified total *ACE2* expression per sample. In line with previous studies[29,30], we found an overall increased expression of both *ACE2* ($P=0.0025$; Extended Data Fig. 4a) and *TMPRSS2* ($P = 0.0002$; Extended Data Fig. 4b) upon SARS-CoV-2 infection. However, anti-hypertensive treatment did not alter *ACE2* expression, in neither patients positive for SARS-CoV-2 nor patients negative for SARS-CoV-2, in line with recent observations from Lee et al.[31].

We conclude that entry factor expression did not predispose ACEI- or ARB-treated patients to SARS-CoV-2 infection. This finding is in accordance with observational studies, which did not reveal any effect of ACEI or ARB treatment on SARS-CoV-2 infection risk in individuals with HT or other CVDs[4].

ARB-treated patients with COVID-19 have a reduced cell-intrinsic antiviral response. We next assessed potential molecular mechanisms that might be involved in the delayed viral clearance of ARB-treated patients within the Pa-COVID-19 cohort described above. Pathway enrichment analysis based on the top 100 genes that were significantly differentially expressed (log fold change > 0.25, false discovery rate (FDR) < 0.05, expression in >10% of cells in one group) in either of the anti-hypertensive treatment groups compared to the HT⁻/CVD⁻ group showed an activation of genes involved in stress and inflammatory response and antigen processing in ciliated cells of ARB⁺ HT⁺/CVD⁺/⁻ patients with COVID-19 (Fig. 3a, Extended Data Fig. 5a and Supplementary Table 4a). For ACEI⁺ HT⁺/CVD⁺/⁻ patients with COVID-19, path-

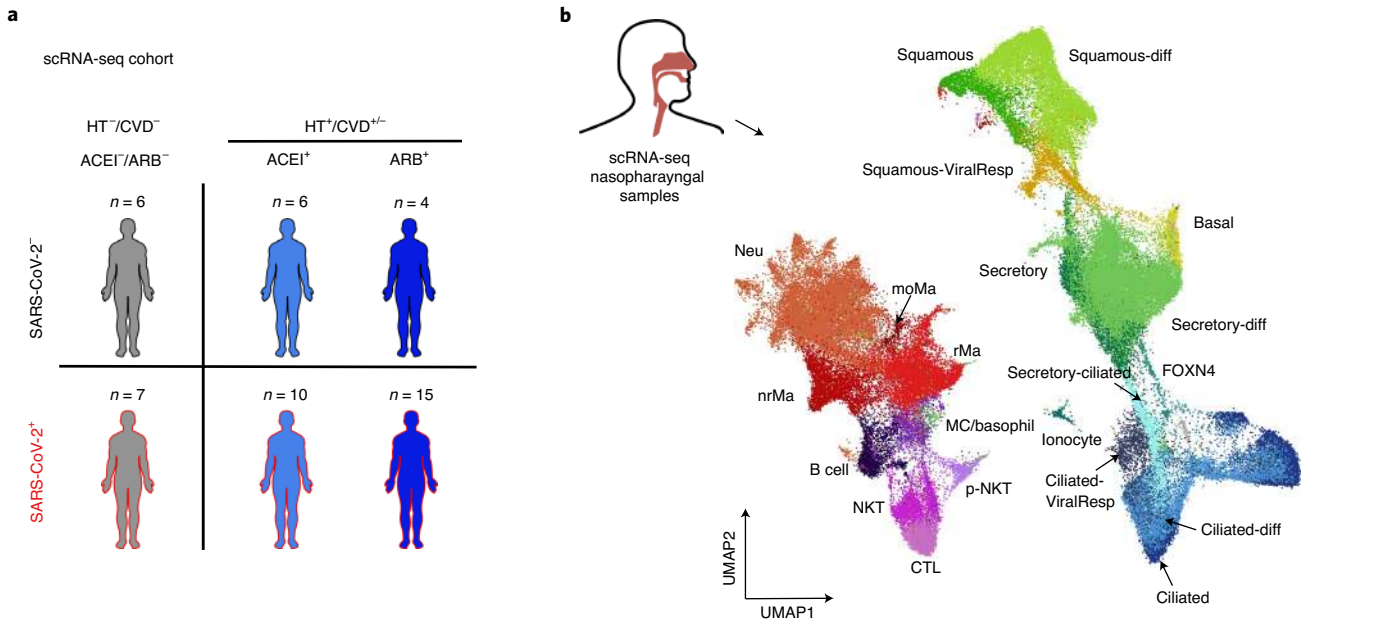

c

Immune cells

	SARS-CoV-2⁻ HT⁻/CVD⁻	SARS-CoV-2⁻ ACEI⁺	SARS-CoV-2⁻ ARB⁺	SARS-CoV-2⁻ HT⁺/CVD⁺/⁻	SARS-CoV-2⁺ HT⁻/CVD⁻	SARS-CoV-2⁺ ACEI⁺	SARS-CoV-2⁺ ARB⁺	SARS-CoV-2⁺ HT⁺/CVD⁺/⁻
B cells	8.75	7.73	9.69	8.37	11.52	3.28*	3.57*	3.61*#
MC/basophil	23.00	28.03	15.31	23.88	6.23#	4.33*#	2.82*#	3.08*#
Neu	21.92	11.82*	13.12	12.24*	45.45#	39.69*#	40.90*#	39.56*#
rMa	7.99	5.00	5.00	5.00	12.04	25.36*#	24.62*	25.49*#
nrMa	6.26	9.09	12.81	10.31	3.50	14.17*	15.03*	14.59*
moMa	0.43	0.00	0.00	0.00	0.38	3.56*#	1.22*#	1.88*#
CTL	8.32	5.45	7.81	6.22	6.28	4.12*	5.06*	5.01*
p-NKT	7.99	7.27	3.44	6.02	2.56#	2.64#	2.39	2.49#
NKT	15.33	25.61*	32.81*	27.96*	12.02	2.85*#	4.39*#	4.29*#

Epithelial cells

	SARS-CoV-2⁻ HT⁻/CVD⁻	SARS-CoV-2⁻ ACEI⁺	SARS-CoV-2⁻ ARB⁺	SARS-CoV-2⁻ HT⁺/CVD⁺/⁻	SARS-CoV-2⁺ HT⁻/CVD⁻	SARS-CoV-2⁺ ACEI⁺	SARS-CoV-2⁺ ARB⁺	SARS-CoV-2⁺ HT⁺/CVD⁺/⁻
Squamous-ViralResp	2.15	2.74	0.91	2.23	4.19#	2.46*	2.9*	2.66*
Squamous	3.06	2.47	1.94	2.32	3.94	4.95	7.39*	6.64*#
Squamous-diff	12.25	14.39	16.29	14.92	10.63#	21.12*	19.77*	21.87*#
Ionocytes	0.29	0.57	0.57	0.57	0.69	0.77	0.61	0.68
Ciliated-ViralResp	3.76	1.94*	14.95*	15.41	1.42#	12.42*	2.54*	3.41*#
Ciliated	17.85	19.78	16.06	18.74	12.58#	10.24*	15.20*	12.09#
Ciliated-diff	9.11	8.57	19.13*	11.52	17.02#	8.14*	17.97	13.40*
FOXN4	0.92	0.04*	0.00*	0.03*	1.61#	0.51*	0.58*	0.60*#
Secretory ciliated	0.45	0.26	0.91	0.45	4.19#	2.05*	3.56	2.77*#
Secretory	15.47	8.08*	7.97*	8.05*	14.32	7.87*	8.13*	8.50*
Secretory-diff	30.54	25.17*	19.59*	23.61*	26.87#	27.75	20.08*	25.69
Basal	4.15	15.98*	2.28	12.15*	2.53#	1.72*	1.29*	1.72#

Fig. 2 | Characteristics of the scRNA-seq cohorts and cell type distribution of nasopharyngeal samples. a, A subset of patients from the Pa-COVID-19 cohort and the SC2-Study were analyzed by scRNA-seq to study the effect of HT/CVD and its treatment by ARB or ACEI in patients negative for SARS-CoV-2 ($n=16$) or positive for SARS-CoV-2 ($n=32$). **b**, Samples were collected from the nasopharynx of the patients and subjected to scRNA-seq, resulting in the given UMAP displaying all identified cell types and states (color coded). **c**, Distribution of epithelial and immune cell types/states in patients negative for SARS-CoV-2 and patients positive for SARS-CoV-2 separated by HT⁺/CVD$^{+/-}$ / HT⁻/CVD⁻ or ACEI⁺/ARB⁺ treatment. Given are percentages related to the total number of epithelial or immune cells, respectively. Benjamini–Hochberg adjusted P values < 0.05 from multinomial logistic regression are given. *Significance compared to HT⁻/CVD⁻; #Significance compared to SARS-CoV-2⁻. CTL, cytotoxic T lymphocyte; diff, differentiating; MC, mast cell; Neu, neutrophil; p-NKT, proliferating natural killer T cell; ViralResp, viral response.

ways related to defense response and regulation of viral genome replication were enriched in ciliated cells. Of those genes involved in regulation of viral genome replication, we found several statistically significantly upregulated type I and type III interferon (IFN)-induced genes (for example, *IFI6*, *IFI27* and *ISG15*; Fig. 3a,b) in both treatment groups.

In secretory cells, ACEI treatment was associated with upregulation of genes negatively regulating immune system response to virus. Interestingly, ARB treatment was associated with a strong induction of genes involved in chemotaxis and inflammatory response in secretory cells (Fig. 3a, Extended Data Fig. 5a and Supplementary Table 4a), including *CXCL1*, *CXCL6* and *IL-8*, which recruit and activate neutrophils (Neu), and *CXCL17*, which is a chemoattractant for monocytes, macrophages and dendritic cells (Fig. 3a,c).

Recently, evidence has been mounting that cell-intrinsic antiviral signaling leading to an early type I/III IFN response plays a substantial role in controlling SARS-CoV-2 replication. Inactivating mutations (single-nucleotide polymorphisms) in key signaling molecules of cell-intrinsic responses (for example, *TRIF*, *TBK1*, *IRF3* and *IRF7*) associate strongly with delayed viral clearance and severe clinical courses of COVID-19 (ref. [32]). Lacking or delayed IFN production, however, can lead to excessive amounts of IFNs late in infection, likely produced by immune cells. This 'extrinsic' IFN signaling appears unable to clear infection and, rather, contributes to inflammation and immune pathology[33,34]. We, therefore, sought to disentangle cell-intrinsic responses triggered by viral infection and cell-extrinsic responses induced by signaling through type I/III IFNs. In an in vitro setting using A549 cells, we studied the extrinsic and intrinsic transcriptional response supposedly induced by SARS-CoV-2 infection. Cells were stimulated either by a highly specific RIG-I ligand triggering prototypical antiviral signaling through IRF3 or by a combination of IFNβ- and INFλ-inducing prototypical IFN signaling through ISGF3 (Fig. 3d). Although the major pattern recognition receptor for SARS-CoV-2 remains elusive, all potential antiviral pathways converge on the transcription factors IRF3/IRF7 and NF-κB[34], eliciting a similar transcriptional response (Supplementary Table 4b).

By overlapping the specific intrinsic and extrinsic antiviral response gene sets identified in the in vitro experiment with the differentially expressed genes in secretory and ciliated cells of patients with COVID-19 (Supplementary Table 4b; for enrichment, see Methods), we observed that overall ACEI but not ARB treatment was associated with a strong cell-intrinsic antiviral response in secretory cells of patients positive for SARS-CoV-2 (Fig. 3e–f and Supplementary Table 4c). Of note, already in patients negative for SARS-CoV-2, anti-hypertensive treatment by ACEI/ARB was associated with the induction of genes involved in cell-intrinsic antiviral defense in secretory but not in ciliated cells (Fig. 3e–f and Supplementary Table 4c). In secretory cells, pre-activation of the intrinsic antiviral response was further enhanced in ACEI-treated $HT^{+}/CVD^{+/-}$ patients with COVID-19 (Fig. 3e). The increase in cell-intrinsic antiviral response was absent in ARB-treated $HT^{+}/CVD^{+/-}$ patients with COVID-19. In the light of recent literature[34], we speculate that this might contribute to an observed delay in SARS-CoV-2 clearance in those patients.

The gene set indicative of extrinsic IFN signaling was not pre-activated in $HT^{+}/CVD^{+/-}$ patients negative for SARS-CoV-2 treated by ACEIs or ARBs. Only upon SARS-CoV-2 infection, a robust extrinsic antiviral response was induced in both ciliated and secretory cells of $HT^{+}/CVD^{+/-}$ patients with COVID-19 treated by ACEIs or ARBs (Fig. 3e,f). A transcription factor binding motif analysis for genes differentially regulated in secretory cells confirmed the notion that the classical cell-intrinsic antiviral signaling through transcription factors such as IRF3, IRF1 and ISGF3 (ISRE) was enriched in $ACEI^{+}$-treated, but not ARB^{+}-treated $HT^{+}/CVD^{+/-}$ patients with COVID-19 (Extended Data Fig. 5b). Instead, ARB^{+}-treated patients showed a strong bias toward genes controlled by NF-κB, which is a hallmark transcription factor for inflammatory conditions[35–37].

Crosstalk between epithelial and immune cells is associated with anti-hypertensive treatment in patients with COVID-19. The differential gene expression by ACEI/ARB described above revealed a distinct induction of inflammatory and chemoattractant genes. Hence, we determined all possible intercellular interactions of all cell types and states across the different conditions using CellPhoneDB[38] (Fig. 4). Basal cells, secretory cells, ciliated cells, resident macrophages (rMa), nrMa, Neu and cytotoxic T lymphocytes (CTL) had the highest number of interactions within the nasopharyngeal mucosa of patients with COVID-19 (Fig. 4a,b). A coexisting CVD correlated with an increased number of cell–cell interactions with most of the previously mentioned cell types, gaining about 500 additional interactions upon SARS-CoV-2 infection (Fig. 4a).

In patients negative for SARS-CoV-2, interactions in $ACEI^{+}$ and ARB^{+} were very similar in number and type (Fig. 4a and Extended Data Fig. 6a). In contrast, for patients with COVID-19, ACEI treatment was concomitant with a reduction of interactions, whereas interactions in ARB treatment remained almost unchanged compared to $HT^{+}/CVD^{+/-}$ patients.

The cell-specific interactions were then categorized as intra- versus inter-compartment interactions (immune:immune and epithelial:epithelial versus immune:epithelial compartment interactions, Extended Data Fig. 6b). In general, regardless of the SARS-CoV-2 infection status, epithelial cells exhibited more potential interactions with themselves, whereas immune cells had more inter-compartment interactions with epithelial cells. When comparing interactions in patients negative for SARS-CoV-2 and patients positive for SARS-CoV-2, we generally observed a loss of intra-compartment interactions for epithelial cells and a gain in inter-compartment interactions with immune cells among all conditions. Both inter- and intra-compartment interactions of immune cells tended to be increased in $HT^{+}/CVD^{+/-}$ patients with COVID-19 compared to HT^{-}/CVD^{-} patients with COVID-19 (Extended Data Fig. 6b and Supplementary Table 5). Accordingly,

Fig. 3 | Differential regulation of antiviral response in patients with different anti-hypertensive treatments. a, Scaled heat maps showing the top 100 genes differentially expressed between SARS-CoV-2^{+} $ACEI^{+}$ or ARB^{+} and HT^{-}/CVD^{-} patients in ciliated and secretory cells by scRNA-seq (scaling by column). Enriched pathways (Extended Data Fig. 5a) and genes shown in **b** are selectively marked next to heat maps. **b**, **c**, Expression plots of genes involved in regulation of viral genome replication in ciliated and secretory cells, respectively. Red circles indicate Benjamini–Hochberg adjusted two-tailed negative binominal $P < 0.05$. Plotting labels on the right side. **d**, Schematic layout of comparative overlap analysis of in vitro experiments (A549 lung cell culture) and scRNA-seq of nasal swaps, displaying the workflow for generation of gene sets used in **e** and **f**. For further details, see Methods. **e**, Bar plots showing the linear fold change of enrichment of overlap between the gene sets generated as shown in **d** (intrinsic and extrinsic, left and right panel, respectively). The differentially regulated gene sets were split into upregulated and downregulated genes, which are displayed separately as positive and negative values on the *x* axis, respectively. Asterisks indicate adjusted *P* values derived from a two-sided hypergeometric test for overlap. For exact *P* values, refer to Supplementary Table 4c. $^{*}P < 0.05$, $^{**}P < 0.01$, $^{***}P < 0.001$. **f**, Iconized table indicating the direction and strength of enrichment shown in **e**. Upward-pointing arrows mark an enriched overlap in upregulated genes (ARB^{+} versus HT^{-}/CVD^{-} and $ACEI^{+}$ versus HT^{-}/CVD^{-}); downward-pointing arrows mark an enriched overlap in downregulated genes. Circles indicate that no significant enrichment of overlap is observed. The numbers of patients cohorts are: SARS-CoV-2^{-} HT^{-}/CVD^{-}: $n = 6$; SARS-CoV-2^{-} $ACEI^{+}$: $n = 6$; SARS-CoV-2^{-} ARB^{+}: $n = 4$; SARS-CoV-2^{+} HT^{-}/CVD^{-}: $n = 7$; SARS-CoV-2^{+} $ACEI^{+}$: $n = 10$; SARS-CoV-2^{+} ARB^{+}: $n = 15$. DEG, differentially expressed gene.

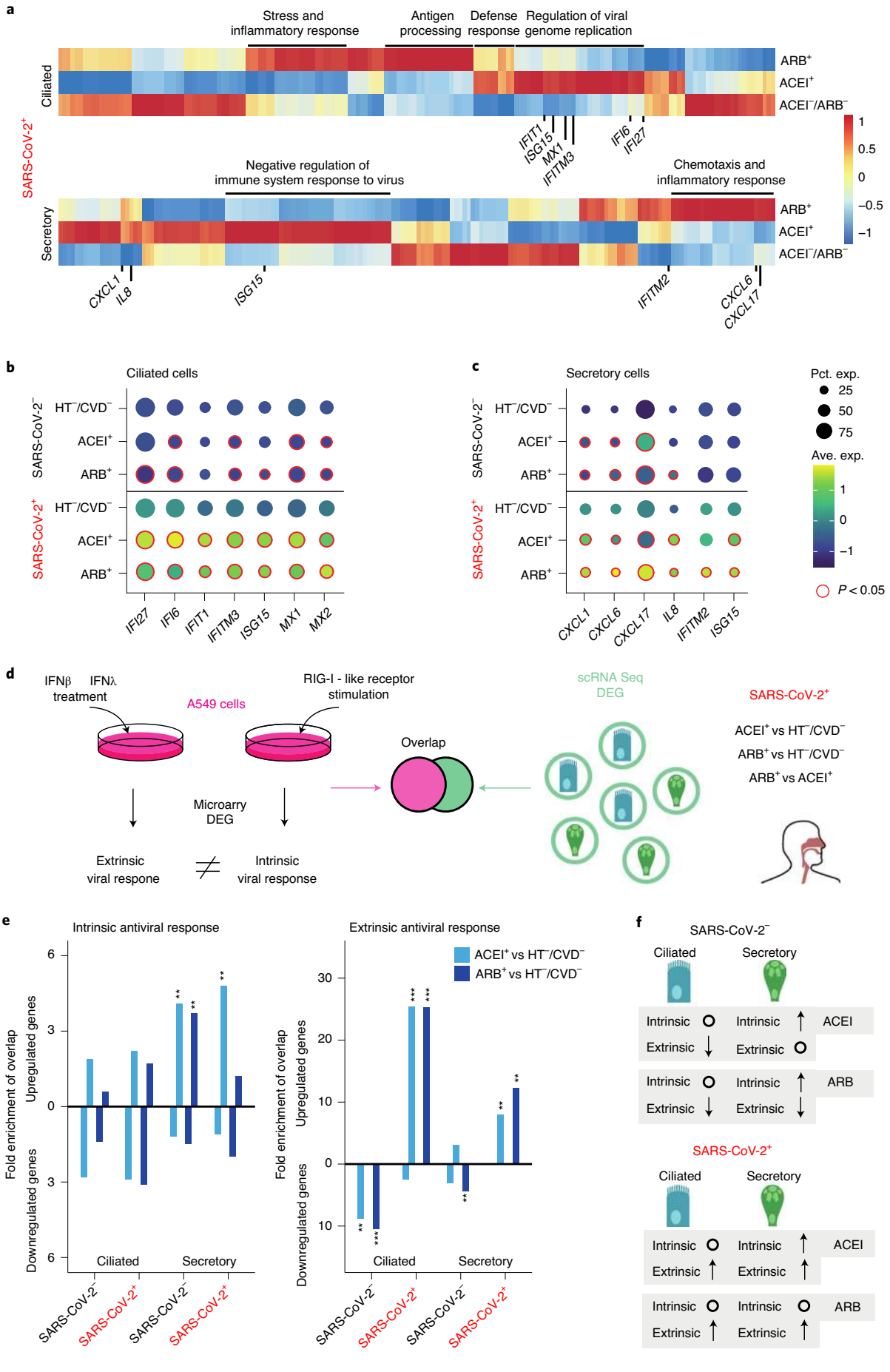
a
Stress and inflammatory response
Antigen processing
Defense response
Regulation of viral genome replication
Ciliated
SARS-CoV-2+
ARB+
ACEI+
ACEI−/ARB−
IFIT1
ISG15
MX1
IFITM3
IFI6
IFI27
Negative regulation of immune system response to virus
Chemotaxis and inflammatory response
Secretory
CXCL1
IL8
ISG15
IFITM2
CXCL6
CXCL17
1
0.5
0
−0.5
−1
b
Ciliated cells
SARS-CoV-2−
SARS-CoV-2+
HT−/CVD−
ACEI+
ARB+
IFI27
IFI6
IFIT1
IFITM3
ISG15
MX1
MX2
c
Secretory cells
CXCL1
CXCL6
CXCL17
IL8
IFITM2
ISG15
Pct. exp.
25
50
75
Ave. exp.
1
0
−1
P < 0.05
d
IFNβ IFNλ treatment
A549 cells
RIG-I - like receptor stimulation
Overlap
Microarry DEG
Extrinsic viral respone
Intrinsic viral response
scRNA Seq DEG
SARS-CoV-2+
ACEI+ vs HT−/CVD−
ARB+ vs HT−/CVD−
ARB+ vs ACEI+
e
Intrinsic antiviral response
Extrinsic antiviral response
Fold enrichment of overlap
Upregulated genes
Downregulated genes
ACEI+ vs HT−/CVD−
ARB+ vs HT−/CVD−
Ciliated
Secretory
SARS-CoV-2−
SARS-CoV-2+
f
SARS-CoV-2−
Ciliated
Secretory
Intrinsic
Extrinsic
ACEI
ARB
SARS-CoV-2+

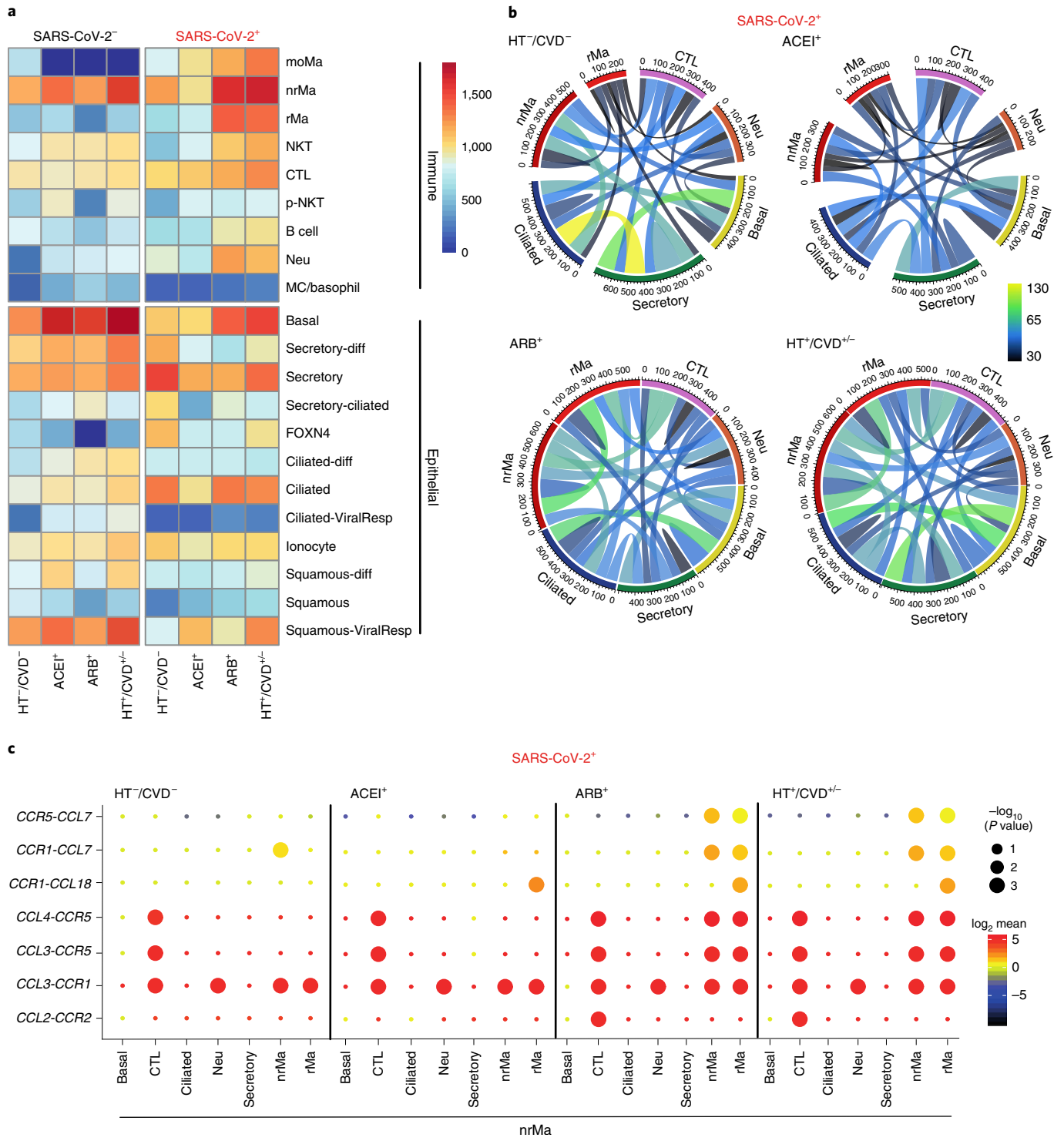

Fig. 4 | Cell–cell interactions in COVID-19 under anti-hypertensive treatment. a, Heat map depicting the total number of interactions per cell type across the different SARS-CoV-2$^{+/-}$ conditions. Scaled by number of identified interactions. All succeeding plots show only SARS-CoV-2^{+} cases. **b**, Circos plots of the most highly interactive cells (basal, secretory, ciliated, CTL, Neu, nrMa and rMa, printed in bold) scaled by the number of identified interactions. **c**, Dot plot showing immune modulatory interactions of nrMa across conditions with the highly interactive cells. Color coding reflects $\log_2$ mean expression, whereas the *P* value derived from CellPhoneDB is shown by the dot size. The patient numbers for deriving the different sets were: SARS-CoV-2^{+} HT^{-}/CVD^{-}: $n=7$; SARS-CoV-2^{+} ACEI^{+}: $n=10$; SARS-CoV-2^{+} ARB+: $n=15$; SARS-CoV-2^{+} HT^{+}/CVD$^{+/-}$: $n=25$; SARS-CoV-2^{-} HT^{-}/CVD^{-}: $n=6$; SARS-CoV-2^{-} ACEI^{+}: $n=6$; SARS-CoV-2^{-} ARB^{+}: $n=4$; SARS-CoV-2^{-} HT^{+}/CVD$^{+/-}$: $n=10$.

intra-compartment interactions upon SARS-CoV-2 infection were exclusively statistically significantly increased in immune cell types but decreased in epithelial cells (Supplementary Table 5).

Notably, this finding was mostly affected by ARB treatment, as ARB^{+}/HT^{+}/CVD$^{+/-}$ patients showed an overall increase in immune cell interactions, whereas ACEI^{+}/HT^{+}/CVD$^{+/-}$ patients were similar

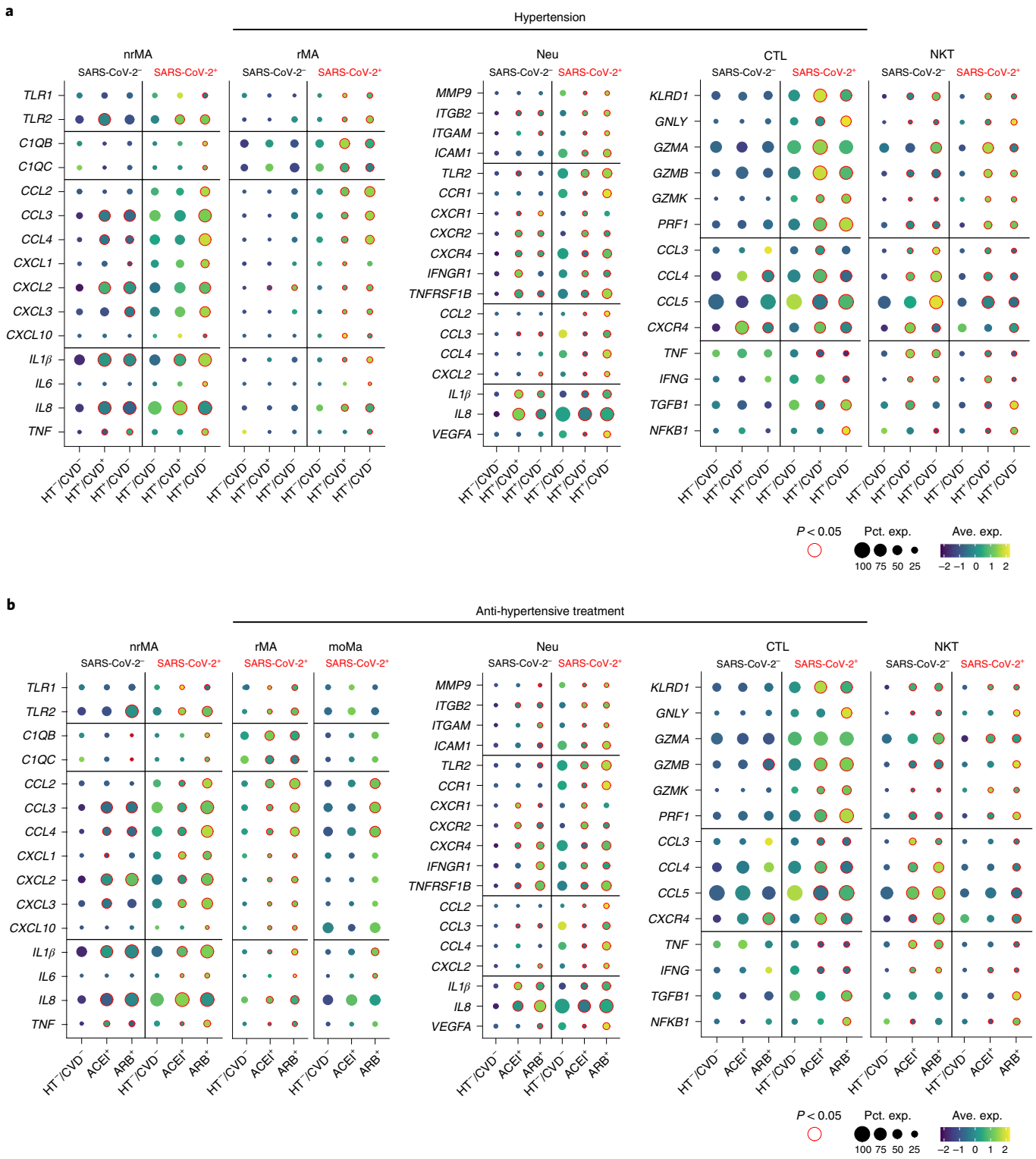

Fig. 5 | Hypertension-related immune response of the upper airway in COVID-19. a, **b**, Dot plots depict gene expression of COVID-19-related pro-inflammatory mediators and receptors in macrophages, neutrophils and T cells of the nasopharynx. **a**, Significant gene expression changes in nrMa, rMa, Neu, NKT and CTL of hypertensive patients with (HT^+/CVD^+, n (SARS-CoV-$2^{+/-}$) = 4/10) or without an additional CVD (HT^+/CVD^-, n (SARS-CoV-$2^{+/-}$) = 6/15) compared to HT^-/CVD^- patients (n (SARS-CoV-$2^{+/-}$) = 6/6). **b**, Significantly altered gene expression in different immune cells of hypertensive patients treated either with ARB^+ (n (SARS-CoV-$2^{+/-}$) = 4/15) or $ACEI^+$ (n (SARS-CoV-$2^{+/-}$) = 6/10) in comparison to HT^-/CVD^- patients (n (SARS-CoV-$2^{+/-}$) = 6/6). Significant differences in **a** and **b** are based on Benjamini–Hochberg adjusted P value calculated using MAST < 0.05 and are indicated by red circles. Samples with no contributing cells per cell type were excluded from analysis. Ave. Exp., average gene expression; Pct. Exp., percentage of cells expressing the gene.

to HT$^-$/CVD$^-$ patients with COVID-19 (Extended Data Fig. 6b and Supplementary Table 5). In particular, chemokine–chemokine receptor interactions mediated by nrMa (Fig. 4c) reflected the similarity between HT$^-$/CVD$^-$ and ACEI-treated patients with COVID-19. HT$^+$/CVD$^{+/-}$ and ARB-treated patients with COVID-19 were similar in their interaction pattern, whereas, in ACEI$^+$, there was a reduced enrichment of interactions between *CCL3/CCL4* and *CCR5* and between *CCR5* and *CCL7*, respectively (Fig. 4c). In line with the pronounced chemokine–chemokine receptor interaction, the expression of *CCL2*, *CCL3*, *CCL4* and *CCL7* was upregulated in ARB$^+$ concomitantly with the expression of their receptors—for example, *CCR1*, *CCR2* and *CCR5*—suggesting a higher interactivity of nrMa under ARB compared to ACEI treatment (Extended Data Fig. 6c).

Hypertension-related inflammatory priming of immune cells is less pronounced in ACEI-treated patients. Hyperinflammation is a hallmark of adverse COVID-19 course[20,21]. Therefore, we evaluated already known key mediators of COVID-19 pathology, including immune cell-recruiting chemokines—for example, *CCL2, CCL3* and *CCL4*—as well as inflammatory cytokines or cytotoxic mediators secreted by T cells, such as *IL1β*, *IL8*, *PRF1* and granzymes. Upon SARS-CoV-2 infection, immune cells of HT$^+$/CVD$^{+/-}$ patients showed a significantly increased expression of these inflammatory mediators compared to HT$^-$/CVD$^-$ patients (Fig. 5a).

When comparing expression of all genes depicted in Fig. 5a between SARS-CoV-2$^+$ HT$^+$/CVD$^{+/-}$/ACEI$^+$ or HT$^+$/CVD$^{+/-}$/ARB$^+$, expression of most genes was significantly enhanced in ARB$^+$ (Fig. 5b and Supplementary Table 6).

For example, in all macrophage subtypes, *CCL3* and *CCL4* expression, as well as the infiltrative potential of Neu (*ITGAM* and *ICAM1*), was increased in HT$^+$/CVD$^{+/-}$/ARB$^+$ compared to HT$^+$/CVD$^{+/-}$/ACEI$^+$ (Fig. 5b and Supplementary Table 6). This hyperinflammatory phenotype was not only present in the upper airways but also in bronchial lavage (BL), as reflected by a stronger activation of BL-nrMa and BL-Neu of a hypertensive patient with COVID-19 (BIH-SCV2-30) compared to an HT$^-$/CVD$^-$ patient (BIH-SCV2-25; Extended Data Fig. 7b).

In the absence of SARS-CoV-2 infection, HT$^+$/CVD$^{+/-}$ patients were characterized by inflammatory priming predominantly in nrMA, Neu and NKT, but not in rMa and CTL, independent of anti-hypertensive treatment (Fig. 5a,b, Supplementary Table 6 and Extended Data Fig. 7a). ACEI treatment, and to a much lesser extent ARB treatment, alleviated the hypertension-related inflammatory response to SARS-CoV-2 infection (Supplementary Table 6).

Exacerbated expression of *CCL3* and *CCL4* observed in ARB-treated hypertensive patients correlates with disease severity. We next evaluated whether the observed hypertension-related inflammatory predisposition of immune cells might contribute to an increased risk for critical COVID-19. All genes showing a hypertension-related inflammatory priming (Supplementary Table 7a) were overlapped with the genes with a significantly increased expression in critical compared to non-critical COVID-19 (Supplementary Table 7b and Fig. 6a). The resulting intersection included three genes, namely *CCL3*, *CCL4* and *CXCR4* (Fig. 6a). Using a logistic regression model considering age, gender, days after onset of symptoms and study center as potential confounding factors, we confirmed a significant positive relationship between expression of *CCL4* derived from nrMa (adjOR/95% CI = 1.04/1.00–1.07, $P = 0.027$) and *CCL3* expressed by Neu (adjOR/95% CI = 1.13/1.01–1.27, $P = 0.02$) with an increased risk for critical COVID-19 (Fig. 6b). Notably, expression of *CCR1*, the receptor bound by *CCL3* and *CCL4*, increased in nrMa and Neu concomitantly with severity of COVID-19, supporting the potential of CCR1 as a therapeutic target[20] (Fig. 6c).

In summary, we conclude that, in contrast to ACEI treatment, ARB therapy was not as efficient in alleviating hypertension-related hyperinflammation, especially in nrMa and Neu, possibly contributing to critical COVID-19 course (Fig. 6d).

Discussion

This study identified potential molecular mechanisms underlying the findings from observational studies that patients with COVID-19 who also had hypertension or cardiovascular disease showed higher morbidity and mortality rates[39–41]. As first-line anti-hypertensive medication includes modulators of RAAS interfering with the pathway employed by SARS-CoV-2 for cellular entry, it has been debated whether ACEI or ARB treatment alters SARS-CoV-2 infectivity and the severity of COVID-19. Our data suggest that the hypertension-associated additional risk for critical disease progression might be reduced by ARB treatment and even more prominently by ACEI treatment. This is corroborated by previous reports observing higher mortality rates in hypertensive patients with COVID-19 in the absence of ACEI/ARB treatment[42].

Several clinical studies are now available comparing SARS-CoV-2 infectivity rates of patients with and without ACEI/ARB treatment[14,43]. Their findings support the notion that testing positive for SARS-CoV-2 is not associated with treatment by ACEI/ARB[14,44]. In line, we observed no difference in *ACE2* expression and initial viral concentration among patient groups. Also, induction of *ACE2* expression after SARS-CoV-2-infection was not altered by ACEI/ARB treatment. However, viral clearance was delayed by ARB therapy. Although reduced viral clearance can be a result of defects in immunity—for example, of an impaired T cell activity—as it has already been reported for cardiovascular diseases[45,46], our data suggest that an altered balance, and potentially timing, of antiviral responses of ciliated and secretory epithelial cells might contribute to delayed viral clearance. We found significantly weaker cell-intrinsic antiviral signaling via IRF3 in ARB-treated compared to ACEI-treated patients, well in line with a recent study reporting a substantial association of genetic loss-of-function variants of genes in that pathway, including IRF3 itself, with severe courses of COVID-19 progression. In contrast, patients under ACEI treatment showed elevated cell-intrinsic antiviral responses and exhibited viral clearance dynamics similar to normotensive patients.

We identified hypertension-associated elevated immunological activity as the prominent factor contributing to the increased risk of hypertensive patients for a more critical course of COVID-19. Hypertensive patients showed an inflammatory predisposition in different immune cell subtypes observed already before SARS-CoV-2 infection, irrespective of anti-hypertensive treatment. Upon SARS-CoV-2 infection, ARB-treated patients exhibited an exaggerated hyperinflammatory response, which was alleviated in ACEI-treated patients. This distinct inflammatory response of patients with COVID-19 under different anti-hypertensive treatments might also give rise to the less pronounced risk reduction for disease severity under ARB compared to ACEI therapy that we observed. We found ACEI treatment potentially rendering neutrophils less invasive compared to ARB treatment in HT$^+$/CVD$^{+/-}$ patients. This parallels results from ischemia–reperfusion data, which showed leukocyte–endothelium interaction inhibited by ACEI treatment, but not ARB treatment, which might result in less neutrophil invasion into lung tissue and, therefore, ameliorating lung injury[47,48]. Furthermore, RAAS dysregulation resulting in decreased Ang(1–7) concentrations might be a central mechanism of COVID-19 pathogenesis[49]. This hypothesis is supported by data from a recent study by Kintscher et al.[50], which showed that SARS-CoV-2 infection significantly decreased Ang(1–7) concentrations, which were restored by ACEI treatment, but not ARB treatment, supporting our notion of a higher anti-inflammatory capacity in ACEI-treated compared to ARB-treated COVID-19 (ref. [50]).

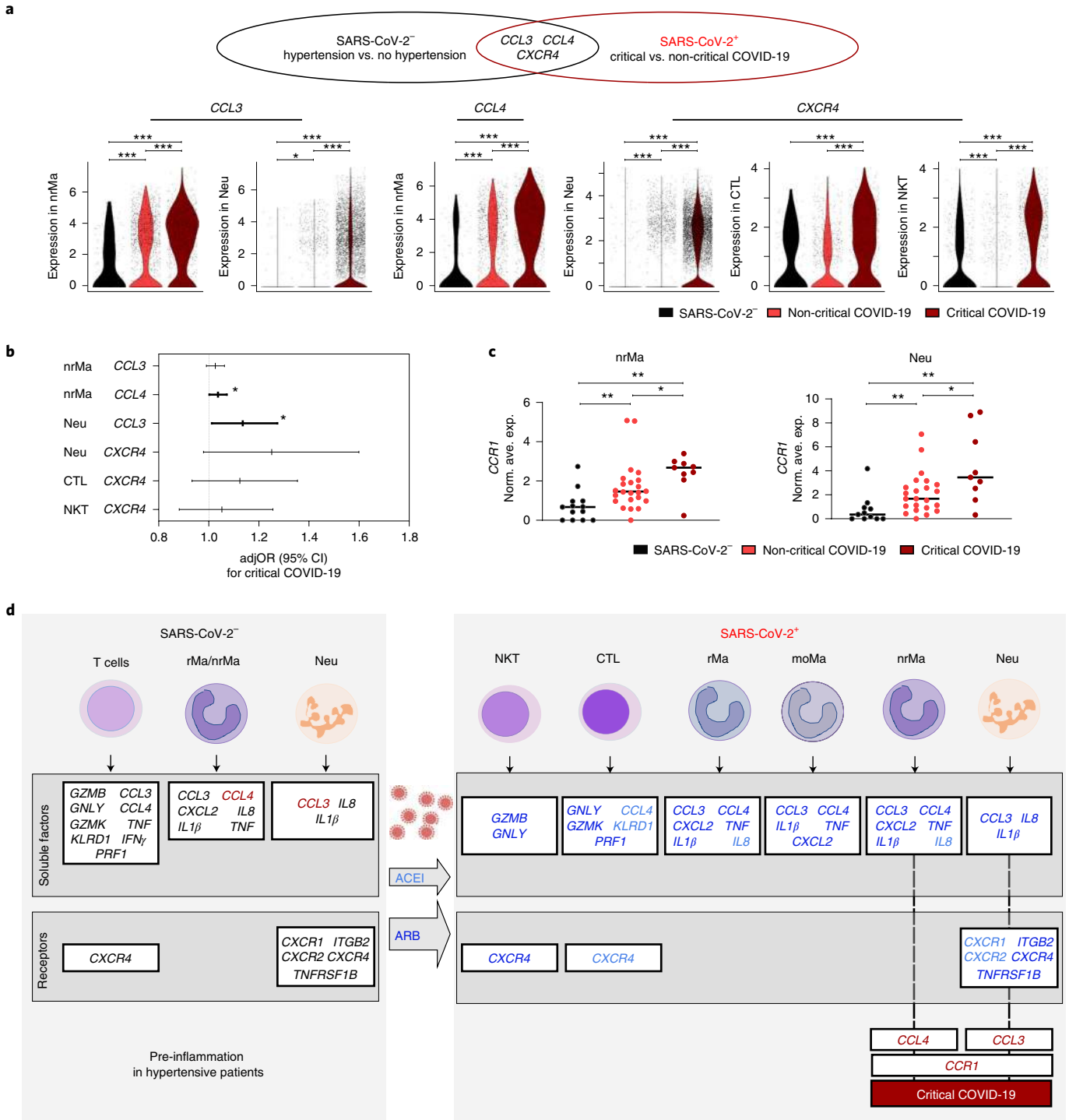

Fig. 6 | Perturbed expression in the *CCL3/CCL4–CCR1* axis correlates with disease severity. a, Schematic layout of the overlay between differentially expressed genes (DEGs) in hypertensive/non-hypertensive patients and DEGs between critical/non-critical patients in all immune cell subtypes. For the genes found in the overlap, violin plots depict expression in patients negative for SARS-CoV-2 and non-critical/critical patients positive for SARS-CoV-2. Significant differences are based on Benjamini–Hochberg adjusted *P* values calculated using MAST. **b**, Adjusted logistic regression analyses of all genes and cell populations found in this overlay in association to critical COVID-19 (confounder: age, gender, days after onset of symptoms and study center). The forest plot shows adjusted odds ratios with whiskers representing the 95% CI. Significant relationships are depicted in bold. **c**, Not only *CCL3* and *CCL4* were significantly associated with severity but also their receptor *CCR1*. Shown are mean expression levels per patient in nrMA and Neu, respectively. Significances were derived from a two-sided Mann–Whitney U test. **d**, The left panel summarizes all genes related to immune mediators and receptors depicted in Fig. 5 that we found to be elevated in $HT^{+}/CVD^{+/-}$ patients negative for SARS-CoV-2 compared to HT^{-}/CVD^{-} patients independent of ACEI/ARB treatment. The right panel shows those genes significantly upregulated in patients positive for SARS-CoV-2 when comparing $ACEI^{+}$ ($n=10$, light blue colored genes) to ARB^{+} ($n=15$, dark blue colored genes). Genes associated with critical COVID-19 are highlighted in red. $^{*}P < 0.05$, $^{**}P < 0.005$, $^{***}P < 0.0005$.

The increased concentrations of Ang(1–7) might reduce the propensity for lung failure and has been suggested as a new therapeutic principle in critical COVID-19 (refs. [51,52]). Animal studies have shown that Ang(1–7) is able to attenuate lipopolysaccharide-induced activation of macrophages, arguing that ACEI might be more beneficial than ARB in reducing the COVID-19-mediated hyperinflammation in this cell population, which has been described as a central feature of adverse COVID-19 (refs. [20,53]). Besides the ACE2/Ang(1–7)/MasR-mediated effects of Ang(1–7)[8,54] it might be also possible that ACEI or ARB treatment increases the concentration of the other anti-inflammatory mediator of the RAAS pathway Ang(1–9). The effects of AT2R activation by Ang(1–9) have been underappreciated in SARS-CoV-2 infection so far, although animal studies on pulmonary hypertension showed its potential to reduce pro-inflammatory mediators such as CCL2 or IL1β[55].

This study demonstrated an immune activation in hypertensive patients that was largely augmented under COVID-19 and might provide an explanation for the adverse course of the disease related to a hyperinflammatory response in these patients. Our data are in line with the general guideline recommendations discouraging discontinuation of ACEI or ARB treatment. In fact, our results might suggest that ACEI could be the more beneficial anti-hypertensive treatment during COVID-19. Although this study is one of the largest single-cell studies of the respiratory system of patients with COVID-19, we have to point out that single-cell RNA sequencing (scRNA-seq) studies are typically restricted to a limited number of patients. Thus, we cannot firmly establish efficacy or study additional potentially interesting confounders, such as the genotype, and other factors, such as co-treatment of patients with the present patient number. As such, randomized controlled trials are required to assess the clinical effect of ACEI versus ARB treatment in patients with COVID-19, and several trials are already under way (for example, NCT04591210, NCT04493359 and DRKS00021732).

Online content

Any methods, additional references, Nature Research reporting summaries, source data, extended data, supplementary information, acknowledgements, peer review information; details of author contributions and competing interests; and statements of data and code availability are available at https://doi.org/10.1038/s41587-020-00796-1.

Received: 16 September 2020; Accepted: 11 December 2020;
Published online: 24 December 2020

References

1. Grasselli, G. et al. Risk factors associated with mortality among patients with COVID-19 in intensive care units in Lombardy, Italy. *JAMA Intern. Med.* **180**, 1345–1355 (2020).
2. Gupta, S. et al. Factors associated with death in critically Ill patients with Coronavirus Disease 2019 in the US. *JAMA Intern. Med.* **180**, 1–12 (2020).
3. Danaei, G. et al. National, regional, and global trends in systolic blood pressure since 1980: systematic analysis of health examination surveys and epidemiological studies with 786 country-years and 5.4 million participants. *Lancet* **377**, 568–577 (2011).
4. Mancia, G., Rea, F., Ludergnani, M., Apolone, G. & Corrao, G. Renin–angiotensin–aldosterone system blockers and the risk of Covid-19. *N. Engl. J. Med.* **382**, 2431–2440 (2020).
5. Liang, X. et al. The association of hypertension with the severity and mortality of COVID-19 patients: evidence based on adjusted effect estimates. *J. Infect.* **81**, e44–e47 (2020).
6. Gao, C. et al. Association of hypertension and antihypertensive treatment with COVID-19 mortality: a retrospective observational study. *Eur. Heart J.* **41**, 2058–2066 (2020).
7. Hoffmann, M. et al. SARS-CoV-2 cell entry depends on ACE2 and TMPRSS2 and is blocked by a clinically proven protease inhibitor. *Cell* **181**, 271–280 (2020).
8. Paz Ocaranza, M. et al. Counter-regulatory renin–angiotensin system in cardiovascular disease. *Nat. Rev. Cardiol.* **17**, 116–129 (2020).
9. Romero, C. A., Orias, M. & Weir, M. R. Novel RAAS agonists and antagonists: clinical applications and controversies. *Nat. Rev. Endocrinol.* **11**, 242–252 (2015).
10. Williams, B. et al. 2018 ESC/ESH guidelines for the management of arterial hypertension. *Eur. Heart J.* **39**, 3021–3104 (2018).
11. Soler, M. J., Barrios, C., Oliva, R. & Batlle, D. Pharmacologic modulation of ACE2 expression. *Curr. Hypertens. Rep.* **10**, 410–414 (2008).
12. Jarcho, J. A., Ingelfinger, J. R., Hamel, M. B., D'Agostino, R. B. Sr. & Harrington, D. P. Inhibitors of the renin–angiotensin–aldosterone system and Covid-19. *N. Engl. J. Med.* **382**, 2462–2464 (2020).
13. Vaduganathan, M. et al. Renin–angiotensin–aldosterone system inhibitors in patients with Covid-19. *N. Engl. J. Med.* **382**, 1653–1659 (2020).
14. Reynolds, H. R. et al. Renin–angiotensin–aldosterone system inhibitors and risk of Covid-19. *N. Engl. J. Med.* **382**, 2441–2448 (2020).
15. Dinh, Q. N., Drummond, G. R., Sobey, C. G. & Chrissobolis, S. Roles of inflammation, oxidative stress, and vascular dysfunction in hypertension. *Biomed. Res. Int.* **2014**, 406960 (2014).
16. Jayedi, A. et al. Inflammation markers and risk of developing hypertension: a meta-analysis of cohort studies. *Heart* **105**, 686–692 (2019).
17. McMaster, W. G., Kirabo, A., Madhur, M. S. & Harrison, D. G. Inflammation, immunity, and hypertensive end-organ damage. *Circ. Res.* **116**, 1022–1033 (2015).
18. Olofsson, P. S. et al. Blood pressure regulation by $CD4^+$ lymphocytes expressing choline acetyltransferase. *Nat. Biotechnol.* **34**, 1066–1071 (2016).
19. Wenzel, U. et al. Immune mechanisms in arterial hypertension. *J. Am. Soc. Nephrol.* **27**, 677–686 (2016).
20. Chua, R.L. et al. COVID-19 severity correlates with airway epithelium-immune cell interactions identified by single-cell analysis. *Nat. Biotechnol.* **38**, 970–979 (2020).
21. Liao, M. et al. Single-cell landscape of bronchoalveolar immune cells in patients with COVID-19. *Nat. Med.* **26**, 842–844 (2020).
22. Benelli, G. et al. SARS-COV-2 comorbidity network and outcome in hospitalized patients in Crema, Italy. Preprint at https://doi.org/10.1101/2020.04.14.20053090 (2020).
23. Liu, S. et al. Clinical characteristics and risk factors of patients with severe COVID-19 in Jiangsu Province, China: a retrospective multicentre cohort study. *BMC Infect. Dis.* **20**, 584 (2020).
24. Richardson, S. et al. Presenting characteristics, comorbidities, and outcomes among 5700 patients hospitalized with COVID-19 in the New York City area. *JAMA* **353**, 2052–2059 (2020).
25. Kurth, F. et al. Studying the pathophysiology of coronavirus disease 2019: a protocol for the Berlin prospective COVID-19 patient cohort (Pa-COVID-19). *Infection* **48**, 619–626 (2020).
26. Lukassen, S. et al. SARS-CoV-2 receptor ACE2 and TMPRSS2 are primarily expressed in bronchial transient secretory cells. *EMBO J.* **39**, e105114 (2020).
27. Ravindra, N.G. et al. Single-cell longitudinal analysis of SARS-CoV-2 infection in human bronchial epithelial cells. Preprint at https://doi.org/10.1101/2020.05.06.081695 (2020).
28. Sungnak, W. et al. SARS-CoV-2 entry factors are highly expressed in nasal epithelial cells together with innate immune genes. *Nat. Med.* **26**, 681–687 (2020).
29. Hou, Y. J. et al. SARS-CoV-2 reverse genetics reveals a variable infection gradient in the respiratory tract. *Cell* **182**, 429–446 (2020).
30. Nawijn, M. C. & Timens, W. Can ACE2 expression explain SARS-CoV-2 infection of the respiratory epithelia in COVID-19? *Mol. Syst. Biol.* **16**, e9841 (2020).
31. Lee, I. T. et al. ACE2 localizes to the respiratory cilia and is not increased by ACE inhibitors or ARBs. *Nat. Commun.* **11**, 5453 (2020).
32. Zhang, Q. et al. Inborn errors of type I IFN immunity in patients with life-threatening COVID-19. *Science* **370**, eabd4570 (2020).
33. Lee, J. S. & Shin, E. C. The type I interferon response in COVID-19: implications for treatment. *Nat. Rev. Immunol.* **20**, 585–586 (2020).
34. Park, A. & Iwasaki, A. Type I and type III interferons - induction, signaling, evasion, and application to combat COVID-19. *Cell Host Microbe* **27**, 870–878 (2020).
35. Liu, T., Zhang, L., Joo, D. & Sun, S.C. NF-κB signaling in inflammation. *Signal Transduct. Target Ther.* **2**, 17023 (2017).
36. Neufeldt, C.J. et al. SARS-CoV-2 infection induces a pro-inflammatory cytokine response through cGAS-STING and NF-κB. Preprint at https://doi.org/10.1101/2020.07.21.212639 (2020).
37. Taniguchi, K. & Karin, M. NF-κB, inflammation, immunity and cancer: coming of age. *Nat. Rev. Immunol.* **18**, 309–324 (2018).
38. Efremova, M., Vento-Tormo, M., Teichmann, S. A. & Vento-Tormo, R. CellPhoneDB: inferring cell-cell communication from combined expression of multi-subunit ligand-receptor complexes. *Nat. Protoc.* **15**, 1484–1506 (2020).
39. Guan, W.J. et al. Comorbidity and its impact on 1590 patients with COVID-19 in China: a nationwide analysis. *Eur. Respir. J.* **55**, 2000547 (2020).
40. Huang, S. et al. COVID-19 patients with hypertension have more severe disease: a multicenter retrospective observational study. *Hypertens. Res.* **43**, 824–831 (2020).

41. Sanyaolu, A. et al. Comorbidity and its impact on patients with COVID-19. *SN Compr. Clin. Med.* 1–8 (2020).
42. Zhang, P. et al. Association of inpatient use of angiotensin-converting enzyme inhibitors and angiotensin II receptor blockers with mortality among patients with hypertension hospitalized with COVID-19. *Circ. Res.* **126**, 1671–1681 (2020).
43. Chung, M. K. et al. SARS-CoV-2 and ACE2: the biology and clinical data settling the ARB and ACEI controversy. *EBioMedicine* **58**, 102907 (2020).
44. Mehta, P. et al. COVID-19: consider cytokine storm syndromes and immunosuppression. *Lancet* **395**, 1033–1034 (2020).
45. Nyambuya, T. M., Dludla, P. V., Mxinwa, V. & Nkambule, B. B. T-cell activation and cardiovascular risk in adults with type 2 diabetes mellitus: a systematic review and meta-analysis. *Clin. Immunol.* **210**, 108313 (2020).
46. Madhur, M. S. & Harrison, D. G. Senescent T cells and hypertension: new ideas about old cells. *Hypertension* **62**, 13–15 (2013).
47. Guba, M. et al. Differential effects of short-term ace- and AT1-receptor inhibition on postischemic injury and leukocyte adherence in vivo and in vitro. *Shock* **13**, 190–196 (2000).
48. Grommes, J. & Soehnlein, O. Contribution of neutrophils to acute lung injury. *Mol. Med.* **17**, 293–307 (2011).
49. Sarzani, R., Giulietti, F., Di Pentima, C., Giordano, P. & Spannella, F. Disequilibrium between the classic renin–angiotensin system and its opposing arm in SARS-CoV-2-related lung injury. *Am. J. Physiol. Lung Cell Mol. Physiol.* **319**, L325–L336 (2020).
50. Kintscher, U. et al. Plasma angiotensin peptide profiling and ACE (angiotensin-converting enzyme)-2 activity in COVID-19 patients treated with pharmacological blockers of the renin–angiotensin system. *Hypertension* **76**, e34–e36 (2020).
51. Klein, N. et al. Angiotensin-(1–7) protects from experimental acute lung injury. *Crit. Care Med.* **41**, e334–e343 (2013).
52. Magalhaes, G. S., Rodrigues-Machado, M. D. G., Motta-Santos, D., Campagnole-Santos, M. J. & Santos, R. A. S. Activation of Ang-(1–7)/Mas receptor is a possible strategy to treat coronavirus (SARS-CoV-2) infection. *Front. Physiol.* **11**, 730 (2020).
53. Souza, L. L. & Costa-Neto, C. M. Angiotensin-(1–7) decreases LPS-induced inflammatory response in macrophages. *J. Cell. Physiol.* **227**, 2117–2122 (2012).
54. Lumpuy-Castillo, J. et al. Cardiovascular damage in COVID-19: therapeutic approaches targeting the renin–angiotensin–aldosterone system. *Int. J. Mol. Sci.* **21**, 6471 (2020).
55. Cha, S. A., Park, B. M. & Kim, S. H. Angiotensin-(1–9) ameliorates pulmonary arterial hypertension via angiotensin type II receptor. *Korean J. Physiol. Pharmacol.* **22**, 447–456 (2018).

Methods

For a brief summary of the study design, applied statistics/software and data availability refer to the Life Sciences Reporting Summary.

Patient recruitment and ethics approval. Patients were enrolled between March 6 and June 7, 2020, in either the prospective observational cohort study Pa-COVID-19 (ref. [25]) at Charité - Universitätsmedizin Berlin or the SC2-Study at the University Hospital Leipzig. Written informed consent was given by all patients or their legal representatives. The study was approved by the respective institutional review boards of the Charité - Universitätsmedizin Berlin (EA2/066/20) or the University Hospital Leipzig (123/20-ek) and conducted in accordance with the Declaration of Helsinki.

Pa-COVID-19 cohort. Between March and May 2020, 162 patients positive for COVID-19 were recruited at Charité - Universitätsmedizin Berlin in the Pa-COVID-19 study. In the study presented here, we excluded those patients who had their positive SARS-CoV-2 test exclusively outside the Charité ($n=12$) and those with missing information on ACEI/ARB treatment ($n=6$). For the remaining 144 patients with COVID-19, we assessed differences in COVID-19 severity related to coexisting cardiovascular diseases (CVD^+), such as hypertension (HT^+/CVD^-) or HT and an additional cardiovascular disease (coronary artery disease and/or heart failure, HT^+/CVD^+) in the different treatment groups ($ACEI^+$, ARB^+ and $ACEIf^-/ARB^-$) compared to patients without HT and CVD (HT^-/CVD^-). HT was defined according to European Society of Cardiology and European Society of Hypertension guidelines as office blood pressure ≥ 140 mm Hg systolic or ≥ 90 mm Hg diastolic[10]. The characteristics of this cohort are summarized in Supplementary Tables 1 and 2.

scRNA-seq cohort. We collected nasopharyngeal swabs for scRNA-seq transcriptome analyses of 32 patients with confirmed COVID-19 (23 males and nine females; median age, 67 years; range, 32–91 years) and 16 controls without any COVID-19-related symptoms (nine males and seven females; median age, 53 years; range, 24–79 years). Relevant patient characteristics are given in Supplementary Table 3.

Of the patients with COVID-19, 23 were classified as having severe disease, and nine were classified as having critical disease, according to World Health Organization (WHO) guidelines[40]. Hospital mortality of these patients was 1/33 (3.0%).

Baseline CVD was prevalent in 25 of the patients with COVID-19. They had HT only ($n=16$, 64%), CVD with HT ($n=7$, 28%) or CVD with heart failure and HT ($n=2$, 8%). Patients with HT only were classified as HT^+, whereas all patients with HT and CVD (and possibly additionally heart failure) were classified as HT^+/CVD^+. Concomitant treatment of $HT^+/CVD^{+/-}$ included treatment with either ACEI ($n=10$) or ARB ($n=15$). Seven of the patients with COVID-19 had no known CVD (21.2%). Note that patient BIH-SCV2-14 was included in all analyses regarding ACEI/ARB treatment but not in the CVD analysis (this patient had HT and heart failure).

Of the symptom-free patients negative for SARS-CoV-2, six had HT only (37.5%), and four had additional CVD (25%). Six of these patients received ACEI (37.5%), and four were treated with ARB (25%). The remaining six patients had no known CVD and, therefore, were treated with neither ACEI nor ARB (37.5%). Only patients with a medically controlled hypertension were included in the cohort.

Isolation and preparation of single cells from human airway specimens, followed by pre-processing of the raw sequencing reads. Sample procurement, single-cell isolation, library preparation and subsequent data analysis were performed as described previously[20]. Briefly, freshly taken nasopharyngeal swabs from donors were directly transferred into 500-µl cold DMEM/F12 medium (Gibco, 11039), and 500 µl of 13 mM DTT (AppliChem, A2948) was added to each sample. Cells were released by gently pipetting the solution onto the swab, followed by dipping the swab 20 times into the medium. Subsequently, the samples were incubated on a thermomixer at 37 °C, 500 r.p.m. for 10 min, followed by centrifugation at 350*g* at 4 °C for 5 min. While carefully removing the supernatant, the pellet was visually examined for any traces of blood. If it contained red blood cells (RBCs), the pellet was resuspended in 500 µl of 1× PBS (Sigma-Aldrich, D8537) and 1 ml of RBC Lysis Buffer (Roche, 11814389001), incubated at 25 °C for 10 min and subsequently centrifuged at 350*g* at 4 °C for 5 min. A single-cell suspension was achieved by resuspending the cell pellet in 500 µl of Accutase (Thermo Fisher Scientific, 00-4555-56), followed by incubation at room temperature for 10 min and gently mixing the cells after 5 min by pipetting. Subsequently, 500 µl of DMEM/F12 supplemented with 10% FBS was added to the cells. After centrifugation at 350*g* at 4 °C for 5 min and removal of the supernatant, the cell pellet was resuspended in 100–500 µl of 1× PBS (depending on the size of the cell pellet). Cell debris was removed by using a 35-µm cell strainer (Falcon, 352235) before cell counting was performed using a disposable Neubauer chamber (NanoEnTek, DHC-N01). The cell suspension was loaded into the 10× Chromium Controller using the 10× Genomics Single Cell 3′ Library Kit version 3.0 (10× Genomics; PN 1000076; PN 1000077; PN 1000078) and 10× Genomics Single Cell 3′ Library Kit version 3.1 (10× Genomics; PN 1000223; PN 1000157; PN 1000213; PN 1000122), and the subsequent reverse transcription, complementary DNA amplification and library preparation was performed according to the manufacturer's instructions. Importantly, we extended the incubation at 85 °C during the reverse transcription to 10 min to ensure virus inactivation. Afterwards, the 3′ RNA sequencing libraries were pooled for either S2 or S4 flow cells (S2: up to eight samples; S4: up to 20 samples) and sequenced on the NovaSeq 6000 Sequencing System (Illumina, paired end, single indexing).

All samples were processed under biosafety S3 within 1 h after procurement. Note that samples not immediately used for library preparation were resuspended in cryopreservation medium (20% FBS (Gibco, 10500), 10% DMSO (Sigma-Aldrich, D8418) and 70% DMEM/F12) and stored at −80 °C. Frozen cells were thawed quickly at 37 °C, pelleted at 350*g* at 4 °C for 5 min and proceeded with normal processing.

Single-cell datasets were processed using cellranger 3.0.1. All transcripts were aligned to a customized human hg19 reference genome (10× Genomics, version 3.1.0) plus the SARS-CoV-2 genome (Refseq-ID: NC_045512) added as an additional chromosome. After alignment, ambient RNA was removed using SoupX[56] using *MUC1*, *MUC5AC* and *MUC5B* as marker genes. Where ambient RNA levels seemed plausible (5–15%), filtered expression matrices were used for downstream analyses.

Further processing was performed using Seurat 3.1.4. Genes were retained if they were present in at least three cells in a sample. Cells with more than or equal to 15% mitochondrial reads or fewer than 200 genes expressed were removed from the analysis. For the number of unique molecular identifiers (UMIs), an upper cutoff was chosen manually per sample based on outliers in a UMI counts versus gene counts plot and was typically in the range of 75,000 to 150,000. After normalizing to 10,000 reads per cell, samples were integrated using stepwise CCA on smaller subsets using 90 components and 2,000 variable genes identified by SelectIntegrationFeatures. On the integrated dataset, principal component analysis (PCA) was run using 90 principal components, followed by Uniform Manifold Approximation and Projection (UMAP) and clustering with a resolution of 2.1, both using all components. NKT, CTL and p-NKT cells were subsetted for further analysis. Scaling, dimensional reduction by PCA and the UMAP were calculated separately for this subset.

Cell types were then refined manually by assessing the expression of known cell type markers. Cell types from epithelial[26,57,58] and immune[59] cell populations were identified according to the expression levels of different marker genes (Extended Data Fig. 2c). The 'viral responsive' cell states of ciliated and squamous epithelial cells (Extended Data Fig. 2b) were identified by gene set enrichment analysis using clusterProfiler version 3.12.0 and the output of 'FindClusters()' function from Seurat as input (https://yulab-smu.github.io/clusterProfiler-book/index.html)[60].

For cell–cell interactions, which are based on the expression of known ligand–receptor pairs in different identified cell types, CellPhoneDB[38] version 2.1.2 was used (https://github.com/Teichlab/cellphonedb). circlize 0.4.10 was used to generate the circos plots to display the cell–cell interactions[61].

Shifts of interactions across the different conditions were tested for significance using a logistic regression based on a binomial distribution (Supplementary Table 5). Arboreto[62] 0.1.5 and pySCENIC[63] 0.10.0 were used to infer transcription factor importance.

Viral load measurement. SARS-CoV-2 RT–PCR results and SARS-CoV-2 RNA concentrations were obtained by using respiratory samples taken for routine testing and by using two different test systems: first, by using an assay targeting the SARS-CoV-2 E-gene as published before[47] and the Roche LC480 instrument; second, by using the cobas SARS-CoV-2 test on the cobas 6800/ 8800 system. In cases of the LC480 system, RNA was extracted by using the MagNA Pure 96 DNA and Viral NA Small Volume Kit on a Roche MagNA Pure 96 system. We quantified SARS-CoV-2 RNA by applying external calibration curves and quantified in vitro transcribed RNA, derived from the E-gene fragment[64], or purified complete SARS-CoV-2 RNA. Viral load (using the E-gene genome target for both test systems) was calculated taking into account different predilutions, extraction volumes and RT–PCR reaction volumes.

Viral load assessment by regression analysis. Data on positive viral messenger RNA (mRNA) measurements were available for 144 patients of the Pa-COVID-19 cohort. To smooth the longitudinal viral mRNA data of each patient, the values were binned in 3-d intervals with respect to the time of the first test result. The maximal value in each bin was considered. In case a patient had a negative test for SARS-CoV-2 between two positive measurements, the negative result was disregarded. Patients for whom only one negative test result was available or had missing confounder information were excluded from the analysis. A linear repeated measurement mixed model assuming a heterogeneous first-order autoregressive structure of the covariance matrix was applied considering ACEI or ARB treatment in comparison to untreated patients without coexisting CVD (otherwise-treated $HT^+/CVD^{+/-}$ patients were excluded) as a fixed effect. The concentration measurements up to the fifth consecutive viral test were included in the model that was adjusted for days after onset of symptoms, gender, BMI, smoking and insulin treatment. Calculations were performed in SPSS version 26. Predicted means were calculated using the maximum likelihood option, and fixed effects were compared by Fisher's least significant difference (LSD).

Slope analysis of viral clearance. To compare the rate of viral clearance among patient groups, we performed a linear fit to viral load measurements during the first 30 d after symptom onset. Zero measurements and patients with fewer than four non-zero measurements within this time frame were excluded from this analysis. Student's *t*-tests were used to identify statistically significant differences in slope among groups.

Identification of RIG-I and type I/III interferon-responsive gene sets. A549 cells were electrotransfected with 400-bp-long in vitro transcribed double-strand RNA (dsRNA)[49] and lysed at 2, 4, 6, 8, 16 and 24 h after transfection or mock electrotransfected and lysed at 2 and 24 h. Alternatively, A549 cells were treated with a mix of 100 IU ml^{-1} of IFNβ (8499-IF-010/CF, R&D Systems) and 2.5 ng ml^{-1} of INFλ-1 (300-02L-100, PeproTech) for 2, 8 or 24 h and then lysed. Total RNA was extracted from cell lysates using the NucleoSpin RNA Plus Kit (Macherey Nagel), and the RNA was subjected to microarray analyses using the Illumina Human HT-12 Expression Beadchip platform at the genomic and proteomics core facility at the German Cancer Research Center. Expression data were quantile normalized; genes with no significant expression at any condition or time point were excluded; and gene regulation at different treatment time points versus the 0-h control was determined using the limma package version 3.33 (Bioconductor). Data were then filtered according to the following criteria to define gene sets.

The gene set 'Cell-intrinsic antiviral (RIG-I-like receptor (RLR)) signaling' comprises genes that were exclusively or predominantly upregulated upon dsRNA transfection (RLR stimulation) but not upon IFN treatment. Although, for the sake of specificity, a very specific RIG-I stimulation was applied, the transcriptional response likely is similar for any antiviral stimulus (for example, through MDA5, STING or TLRs) that activates the IRF3 transcription factor. The cutoffs were as follows: maximum (at any time point) $\log_2$ fold change in dsRNA-transfected samples (maximum $\log_2$ FC-RNA) > 2.0 and maximum $\log_2$ fold change in IFN-treated samples (maximum $\log_2$ FC-IFN) < 1.0; genes were excluded as electrotransfection artifacts if maximum log2 fold change in mock transfection (maximum $\log_2$ FC-mock) > 0.5 × (maximum $\log_2$ FC-RNA − maximum $\log_2$ FC-IFN) (11 genes). This procedure yielded a list of 238 genes, comprising expected genes such as the IRF3-dependent type I and III IFN genes themselves (*IFNB1* and *IFNL1*, *IFNL2* and *IFNL3*) and classical NF-κB targets such as *TNFAIP3* (previously *A20*) and the IκB genes *NFKBIA*, *NFKBIB* and *NFKBIZ*.

The gene set 'Extrinsic/paracrine type I/III IFN signaling' comprises genes that were strongly upregulated by extrinsic IFNβ/INFλ treatment whereas less so by cell-intrinsic RLR induction. Note that most IFN-induced genes were upregulated by RLR signaling as well, putatively due to the above-noted IFN production upon RLR stimulation. We enriched this gene set for genes with a bias toward IFN and against RLR signaling by applying the below-described filters. Notably, a few genes, such as *LY6E*, described to possess antiviral activity against SARS-CoV-2 (ref. [50]), were induced only upon IFN treatment but not at all by RLR signaling. In general, we found less profound gene induction in IFN-treated conditions than in dsRNA-transfected conditions, likely due to the moderate dose of IFN used; we, therefore, used less stringent cutoffs for this gene set: maximum $\log_2$ FC-IFN > 0.8 and (maximum $\log_2$ FC-IFN − maximum $\log_2$ FC-RNA) > −0.5. The latter filter removed roughly 50% of the genes, selecting for those with a relative bias of IFN treatment over dsRNA transfection. Filtering yielded 95 genes, including many of the well-known *ISGF3*-driven IFN-stimulated genes (ISGs), including the MX family genes *IFIT1*, *IFITM2*, *IFITM3* and *ISG15*. Both gene sets are included as Supplementary Table 4b.

Statistics. Differences in the percentage of *ACE2*-expressing cells were calculated using logistic regression in R 3.6.1. 95% CIs for the percentage of *ACE2*-expressing cells are provided. Differences in gene expression were calculated using 'FindMarkers()' in Seurat version 3.1.4 with the MAST-based differential expression test adjusted for days after symptom onset[65]. Overlap statistics were calculated as hypergeometric tail probabilities. Differences in CPM were calculated using an analysis of variance (ANOVA) followed by Tukey's honest significance of differences test after assessing homoskedasticity using Bartlett's test. When multiple tests were performed, *P* values were adjusted using the Benjamini–Hochberg method. Total CPM values were extracted from the filtered and raw matrices output by CellRanger. Motif enrichment *P* values were calculated using HOMER 4.10.0 (ref. [66]). To analyze the potential contribution of HT/CVD and its treatment on COVID-19 severity in the Pa-COVID-19 cohort, we conducted chi-square tests and logistic regression models adjusted for gender, BMI, insulin treatment and number of co-treatments with statins, calcium channel blockers or beta blockers. Age showed collinearity with ACEI or ARB treatment. Therefore, age was omitted as a confounder in models where ACEI or ARB treatment was used as an independent variable. Viral clearance was assessed based on similarly adjusted linear regression models as described above. Logistic regression models assessing gene expression changes observed in the scRNA-seq cohort were adjusted for age, gender, days after symptom onset and study center. Blood pressure values passed the tests for normality and were, therefore, analyzed by a two-tailed *t*-test or a one-way ANOVA. Mean expression per patient was analyzed by the Mann–Whitney U test. These analyses were conducted using Statistica version 13.3 (TIBCO Software).

Reporting Summary. Additional information on research design is available in the Nature Research Reporting Summary linked to this article.

Data availability

Due to potential risk of de-identification of pseudonymized scRNA-seq data, the raw data will be available under controlled access in the European Genome-phenome Archive repository (EGAS00001004772). Count and metadata tables (patient ID, sex, age, cell type and quality control metrics per cell) can be found at FigShare: https://doi.org/10.6084/m9.figshare.13200278. In addition, these data can be further visualized and analyzed in the Magellan COVID-19 data explorer at https://digital.bihealth.org. Besides newly generated and unpublished single-cell transcriptome data of 31 patients, we also re-analyzed single-cell transcriptome data of 17 previously published patients (EGAD00001006339)[20], focusing on and addressing different biomedical questions. The human hg19 reference genome (version 3.1.0) or the SARS-CoV-2 genome (Refseq-ID: NC_045512) used in this study can be found at https://cf.10xgenomics.com/supp/cell-exp/refdata-cellranger-hg19-3.0.0.tar.gz or https://www.ncbi.nlm.nih.gov/nuccore/1798174254, respectively.

Code availability

No custom code was generated or used in this study.

References

56. Young, M. & Behjati, S. SoupX removes ambient RNA contamination from droplet based single-cell RNA sequencing data. Preprint at https://www.biorxiv.org/content/10.1101/303727v1 (2020).
57. Plasschaert, L. W. et al. A single-cell atlas of the airway epithelium reveals the CFTR-rich pulmonary ionocyte. *Nature* **560**, 377–381 (2018).
58. Vieira Braga, F. A. et al. A cellular census of human lungs identifies novel cell states in health and in asthma. *Nat. Med.* **25**, 1153–1163 (2019).
59. Travaglini, K. J. et al. A molecular cell atlas of the human lung from single-cell RNA sequencing. *Nature* **587**, 619–625 (2020).
60. Yu, G., Wang, L. G., Han, Y. & He, Q. Y. clusterProfiler: an R package for comparing biological themes among gene clusters. *OMICS* **16**, 284–287 (2012).
61. Gu, Z., Gu, L., Eils, R., Schlesner, M. & Brors, B. Circlize implements and enhances circular visualization in R. *Bioinformatics* **30**, 2811–2812 (2014).
62. Moerman, T. et al. GRNBoost2 and Arboreto: efficient and scalable inference of gene regulatory networks. *Bioinformatics* **35**, 2159–2161 (2019).
63. Aibar, S. et al. SCENIC: single-cell regulatory network inference and clustering. *Nat. Methods* **14**, 1083–1086 (2017).
64. Corman, V. M. et al. Detection of 2019 novel coronavirus (2019-nCoV) by real-time RT–PCR. *Euro. Surveill.* **25**, 2000045 (2020).
65. Finak, G. et al. MAST: a flexible statistical framework for assessing transcriptional changes and characterizing heterogeneity in single-cell RNA sequencing data. *Genome Biol.* **16**, 278 (2015).
66. Heinz, S. et al. Simple combinations of lineage-determining transcription factors prime cis-regulatory elements required for macrophage and B cell identities. *Mol. Cell* **38**, 576–589 (2010).

Acknowledgements

We thank all patients from the Pa-COVID-19 and the SC2 cohort studies for kindly donating nasopharyngeal samples and clinical data. We also thank A. Krannich and Charité - Universitätsmedizin Berlin for help in sample procurement and annotation and for supporting sample processing, respectively. We thank A. Seidel and G. Szczepankiewicz for supporting patient recruitment at the University Hospital Leipzig. We thank H. G. Kräusslich for initial discussions, as well as C. Spann and D. Schweinoch for their help with the in vitro experiment. M.T.V. holds a scholarship from the Clinician Scientist Program of the University of Leipzig, Medical Faculty. M.S.A. has received research support from the German Cardiovascular Research Center. This study was supported by the BIH COVID-19 research program (C.G., C.C., C.D., N.I., L.-E.S., R.E. and I.L.), the European Commission (ESPACE, 874719, Horizon 2020, C.C. and R.E.), the BMBF-funded de.NBI Cloud within the German Network for Bioinformatics Infrastructure (de.NBI; 031A537B, 031A533A, 031A538A, 031A533B, 031A535A, 031A537C, 031A534A and 031A532B, J.E. and R.E.), the BMBF-funded Medical Informatics Initiative (HiGHmed, 01ZZ1802A - 01ZZ1802Z, R.E.) and OrganoStrat (01KX2021, C.G.). We thank Illumina GmbH for financial support via the allocation of reagents and sequencing flow cells, as well as M. Vossmann, M. Allgaier and O. Krätke for the realization of the sequencing runs at the Illumina Solutions Center Berlin. We thank B. Timmermann and his team for the realization of the sequencing runs at the MPI for Molecular Genetics Berlin. This publication is part of the Human Cell Atlas (www.humancellatlas.org/publications).

Author contributions

R.E., C.C., U.L. and I.L. conceived, designed and supervised the project. V.M.C. and C.D. performed qPCR experiments and/or provided the data. S. Trump, S. Lukassen, R.L.C. L.T., J. Liebig, T.K., C.K., T.B. and J.S. performed data analysis. J. Liebig, R.L.C., J. Loske and M.M. performed the single-cell RNA sequencing experiments. M.B. performed and analyzed the in vitro experiment. J. Loske, C.K., M.M., J.K. and F.P. provided

experimental support. M.S.A, S.H., A.L., B.H., F.K., M.W., M.T.V., S.D.M, U.G.L., L.-E.S. and S. Laudi provided the human specimens, clinical data and annotation of the patients. S. Trump and B.P.H. managed patient data of the cohort. S. Twardziok, J.P.A. and J.E. provided technical and data management support. S. Twardziok developed Magellan. B.P.H., C.G., N.I., L.K. and U.L. contributed with discussion of the results. S. Trump, S. Laudi, S. Lukassen, R.L.C., L.T., B.P.H., R.E. and I.L. wrote and prepared the manuscript. All authors read, revised and approved the manuscript.

Competing interests

M.S.A. has received personal fees from Servier outside of the submitted work. All other authors do not declare any competing interests.

Additional information

Extended data is available for this paper at https://doi.org/10.1038/s41587-020-00796-1.

Supplementary information is available for this paper at https://doi.org/10.1038/s41587-020-00796-1.

Correspondence and requests for materials should be addressed to S.L., R.E., C.C., U.L. or I.L.

Peer review information *Nature Biotechnology* thanks Sergio Lavandero, Sylvia Knapp, John Alcorn and Ivo Gut for their contribution to the peer review of this work.

Reprints and permissions information is available at www.nature.com/reprints.

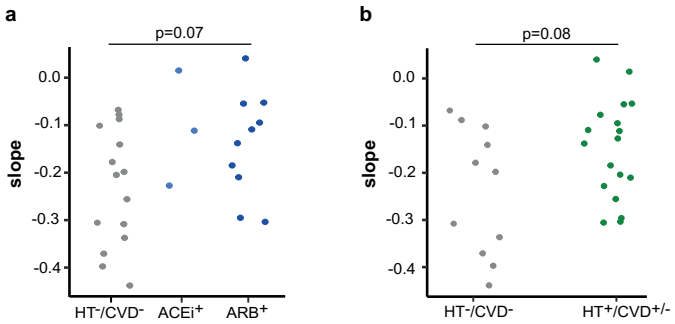

Extended Data Fig. 1 | Slope analyses of viral clearance for Pa-COVID-19 patients. Slope analyses (**a**) of the viral clearance related to ACEI or ARB treatment and (**b**) in in relation to hypertension. CVD= cardiovascular disease, HT=hypertension, p-values (p) from two-sided Student's t-test.

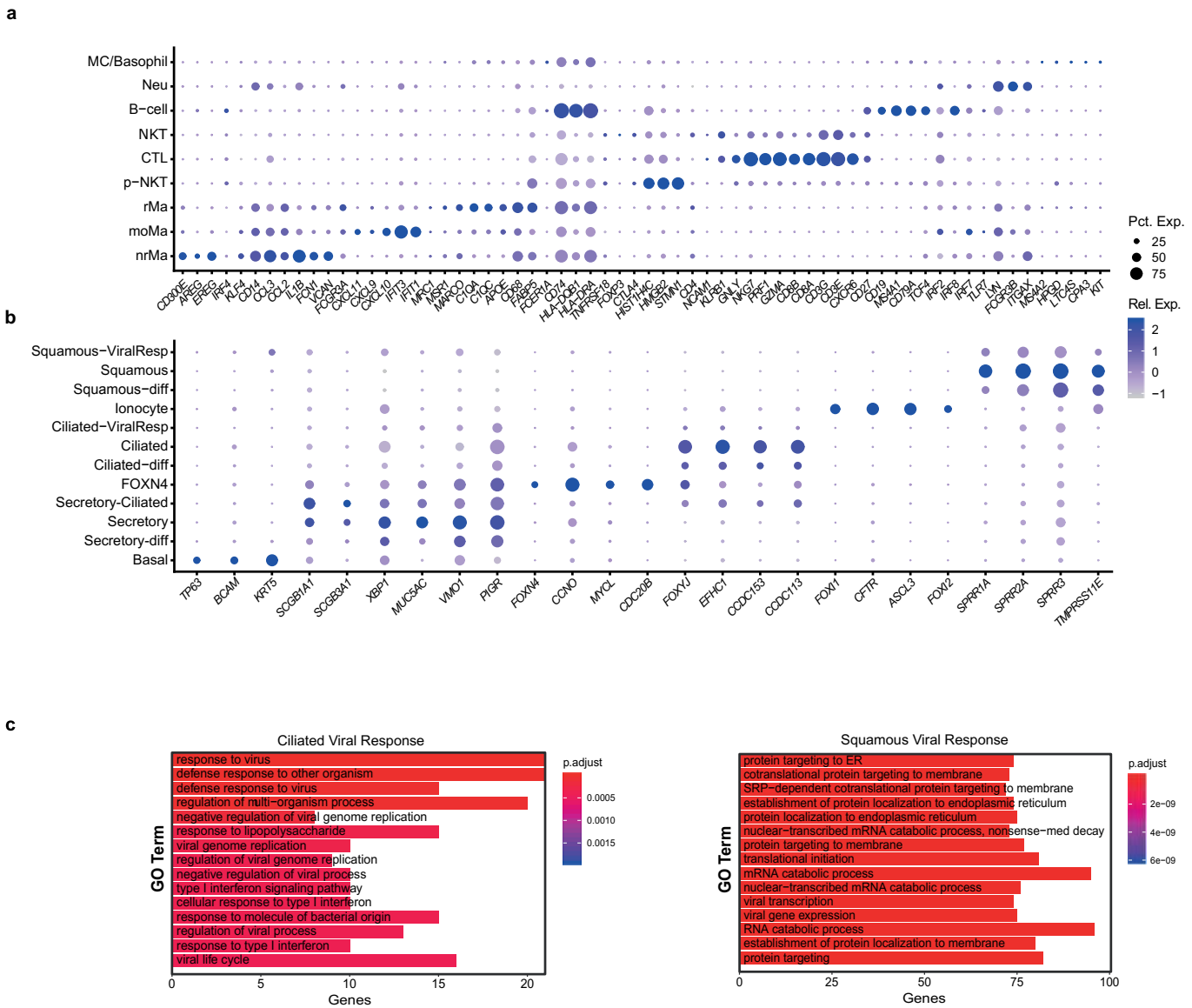

Extended Data Fig. 2 | Cell type characteristics of the scRNA-seq cohort. a, Dotplot depicting marker genes used to identify immune cell types. **b**, Dotplot depicting marker genes of epithelial cell types. For dotplots, expression levels are color-coded and the percentage of cells expressing a respective gene is size-coded. **c**, GO-term enrichment for differentially expressed genes in the ciliated and squamous ViralResp cell cluster. Number of genes observed per term are depicted, adjusted p-values were calculated by the GSEA method with clusterProfiler and indicated by colour.

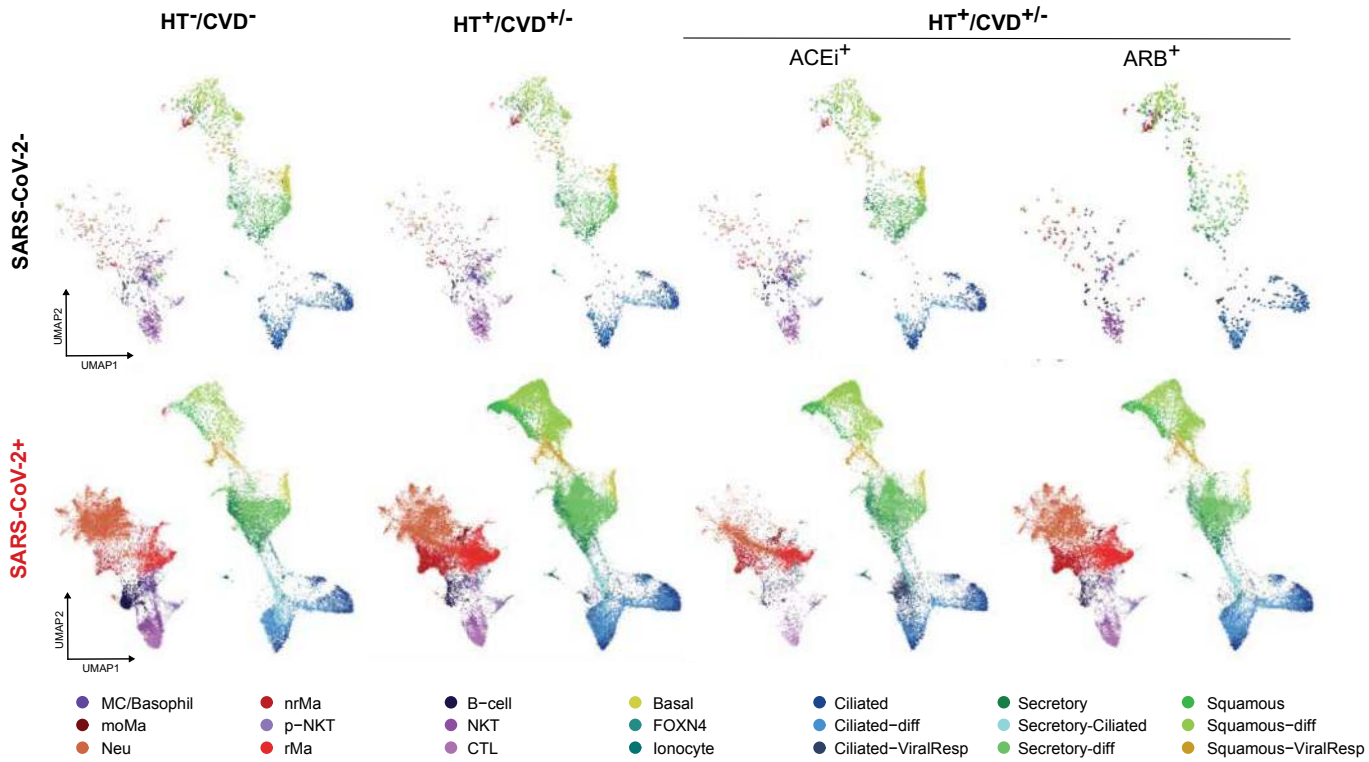

Extended Data Fig. 3 | Cell type distribution in the scRNA-seq cohort. UMAPs depicting distribution of cell types and states in SARS-CoV-2 negative and positive patients. UMAPs are presented separately for controls (HT^{-}/CVD^{-}), patients with a pre-existing cardiac disease ($HT^{+}/CVD^{+/-}$) and the treatment there of ($ACEI^{+}$ and ARB^{+}, respectively). UMAP=uniform manifold approximation and projection, MC=mast cells; moMa = monocyte derived macrophage; Neu = neutrophil; (n)rMa=(non-)resident macrophage; p-NKT=proliferating natural killer T-cell; CTL=cytotoxic T lymphocyte; diff = differentiating; ViralResp = viral response.

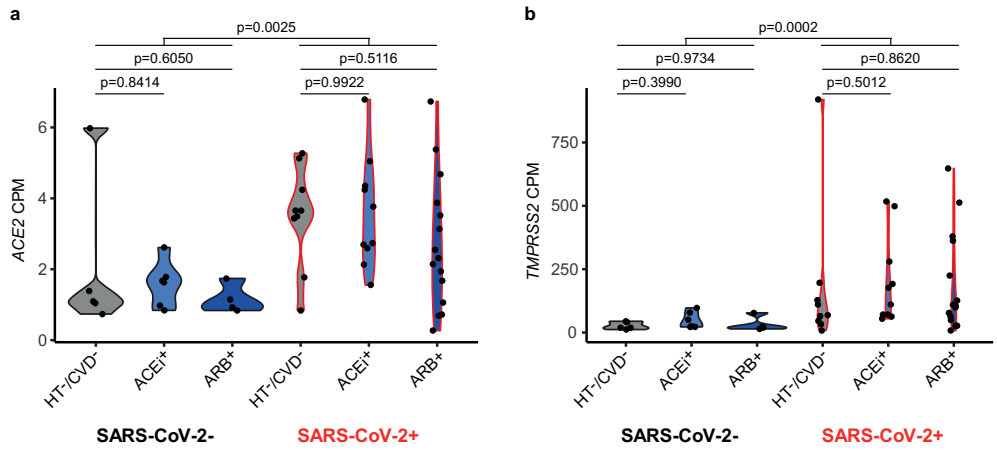

Extended Data Fig. 4 | *ACE2* and *TMPRSS2* expression. Violin plots showing the total *ACE2* and *TMPRSS2* expression per sample in counts per million, split by treatment and infection group. Tukey's p-values for two-sided individual comparisons are shown. The patient numbers for the different sets were: SARS-CoV-2^{-} HT^{-}/CVD^{-}: n = 6; SARS-CoV-2^{-} ACEI^{+}: n = 6; SARS-CoV-2^{-} ARB^{+}: n = 4; SARS-CoV-2^{+} HT^{-}/CVD^{-}: n = 8; SARS-CoV-2^{+} ACEI^{+}: n = 10; SARS-CoV-2^{+} ARB^{+}: n = 15.

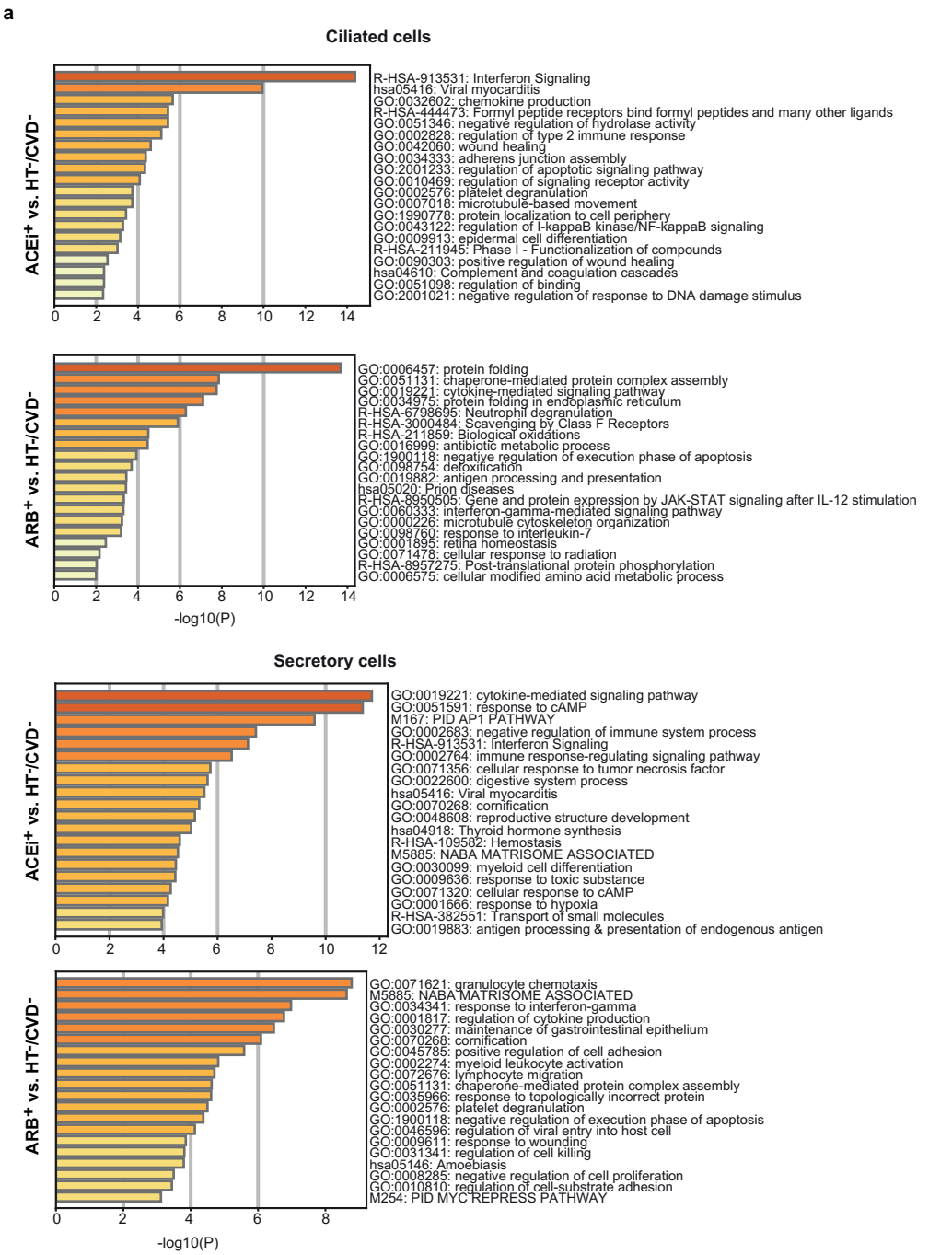

Extended Data Fig. 5 | See next page for caption.

Extended Data Fig. 5 | Pathway and transcription factor binding motif enrichment analysis. a, Pathway enrichment analysis of gene sets (compare Fig. 3a) specific to the condition indicated to the right of each panel in ciliated (two upper panels) and secretory cells (two lower panels) in COVID-19 patients. **b**, Heatmap showing the p-values of a motif-enrichment analysis for the gene sets upregulated in secretory cells of ACEI$^+$ or ARB$^+$ vs. HT$^-$/CVD$^-$ COVID-19 patients. Linear Bonferroni-corrected p-values derived from one-sided hypergeometric tests are indicated as labels, $\log_{10}$ p-values are used for color-coding. The patient numbers for deriving the different sets were: SARS-CoV-2$^+$ HT$^-$/CVD$^-$: n = 8; SARS-CoV-2$^+$ ACEI$^+$: n = 10; SARS-CoV-2$^+$ ARB$^+$: n = 15.

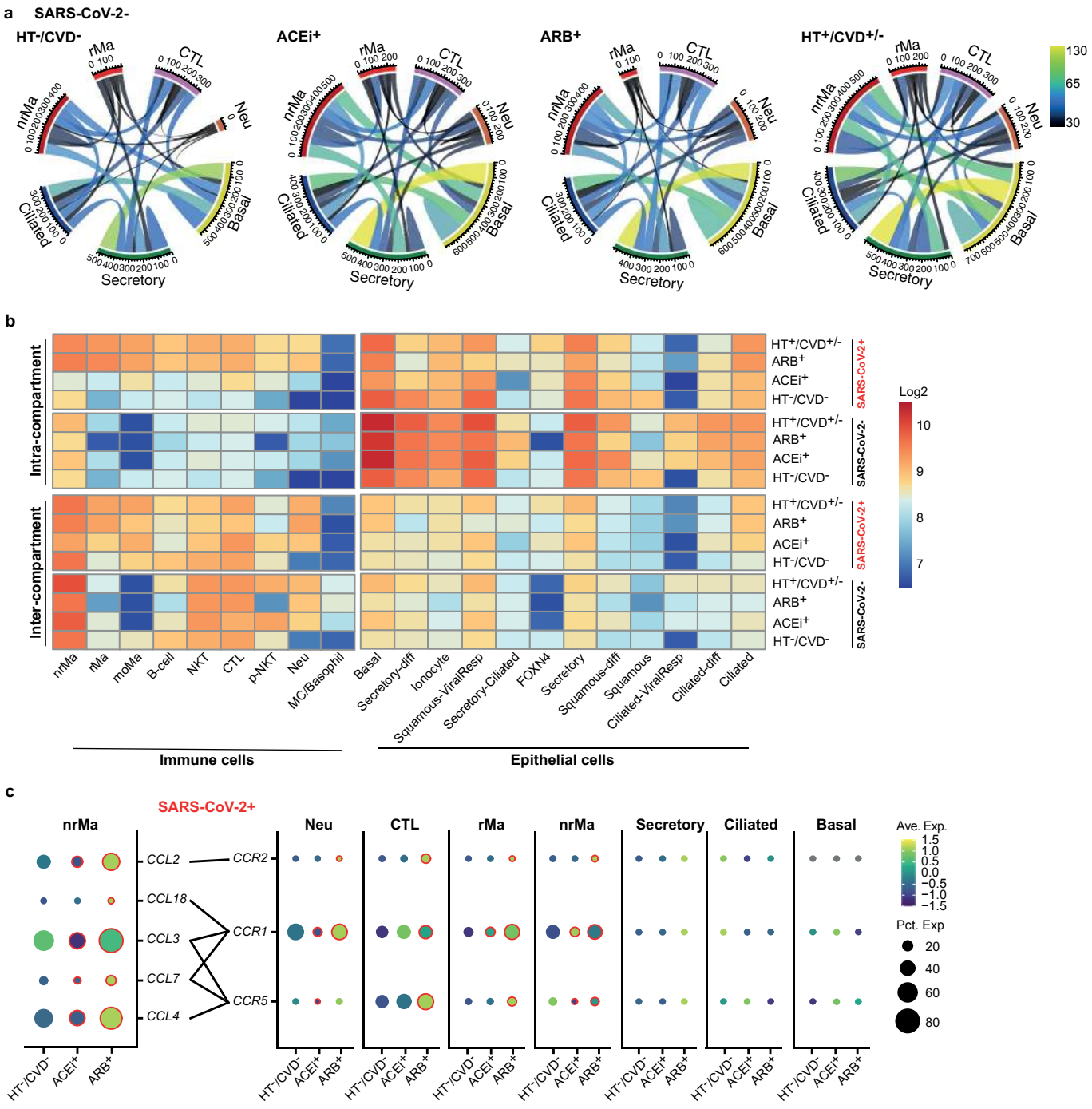

Extended Data Fig. 6 | Cell-cell interactions in SARS-CoV-2 negative patients. a, Circos plots of highly interactive cells (basal, secretory, ciliated, CTL, Neu, nrMa, and rMa). Scaled by the number of identified interactions. **b**, Heatmap showing interactions per cell type categorized as inter-/intra-compartment interactions for SARS-CoV-2 positive and negative cohorts. Log_2 scaling of the number of identified interactions. Significance was measured by a logistic regression model on a binomial distribution (Supplementary Table 5). **c**, Dotplot showing the expression profile of the different immune modulatory factors by the highly interactive cells. Expression levels are color coded; the percentage of cells expressing the respective gene is size coded. Significantly altered expression (Benjamini–Hochberg adjusted two-tailed, negative-binomial $P < 0.05$) in ACEI$^+$ versus HT-/CVD- (circles around ACEI$^+$) and ARB$^+$ versus HT$^-$/CVD$^-$ (circles around ARB$^+$) is marked by a red circle. Ave. Exp. = average expression, Pct. Exp. = percentage of cells expressing the gene. The patient numbers for deriving the different sets were: SARS-CoV-2$^-$ HT$^-$/CVD$^-$: n = 6; SARS-CoV-2$^-$ ACEI$^+$: n = 6; SARS-CoV-2$^-$ ARB$^+$: n = 4; SARS-CoV-2$^-$ HT$^+$/CVD$^{+/-}$: n = 10; SARS-CoV-2$^+$ HT$^-$/CVD$^-$: n = 7; SARS-CoV-2$^+$ ACEI$^+$: n = 10; SARS-CoV-2$^+$ ARB$^+$: n = 15; SARS-CoV-2$^+$ HT$^+$/CVD$^{+/-}$: n = 25.

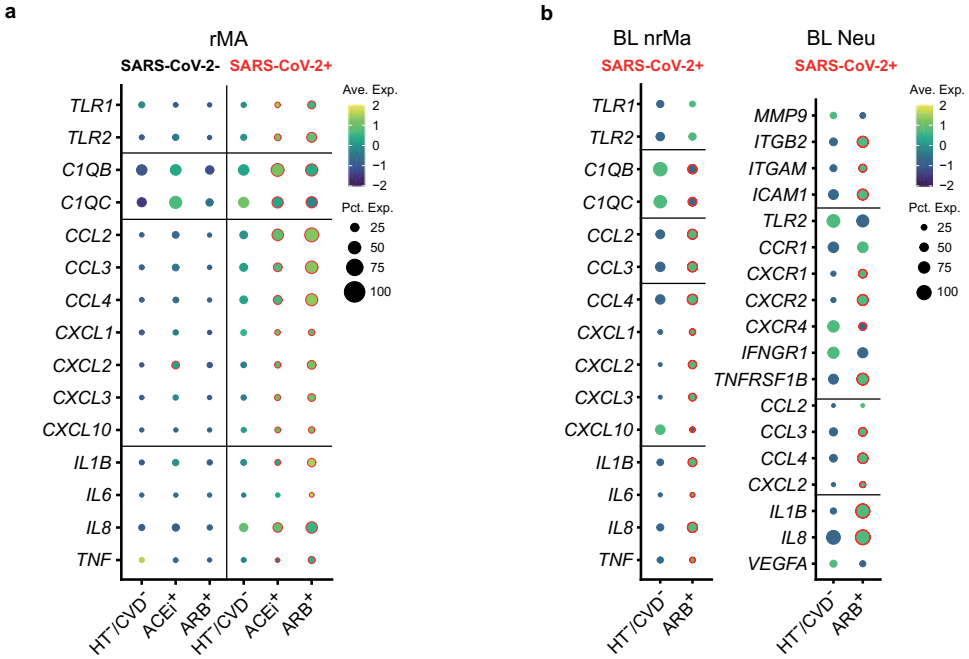

Extended Data Fig. 7 | Immune response in SARS-CoV-2 negative and COVID-19 patients in relation anti-hypertensive treatment. a, Dotplot depicts significant gene expression changes of pro-inflammatory mediators, and receptors in rMa of hypertensive patients treated either with ARB$^+$(n (SARS-CoV-2$^{-/+}$) = 4/15), or ACEI$^+$ (n (SARS-CoV-2$^{-/+}$) = 6/10) in comparison to HT$^-$/CVD$^-$ patients (n (SARS-CoV-2$^{-/+}$) = 6/6). **b**, Shown are gene expression alterations in nrMa and Neu obtained from the bronchial lavage of the COVID-19 HT$^+$/CVD$^+$/ARB$^+$ patient (BIH-SCV2-30) and the HT$^-$/CVD$^-$ patient (BIH-SCV2-25). Red circles indicate Benjamini-Hochberg adjusted two-tailed negative binominal *p*-value<0.05 calculated using MAST. Samples with no contributing cells per cell type were excluded from analysis. Ave. Exp. = average expression, Pct. Exp. = percentage of cells expressing the gene. BL=bronchial lavage.

nature research

Corresponding author(s): Sven Laudi, Roland Eils, Christian Conrad, Ulf Landmesser, Irina Lehmann

Last updated by author(s): Dec 11, 2020

Reporting Summary

Nature Research wishes to improve the reproducibility of the work that we publish. This form provides structure for consistency and transparency in reporting. For further information on Nature Research policies, see Authors & Referees and the Editorial Policy Checklist.

Statistics

For all statistical analyses, confirm that the following items are present in the figure legend, table legend, main text, or Methods section.

n/a	Confirmed	
☐	☒	The exact sample size (*n*) for each experimental group/condition, given as a discrete number and unit of measurement
☐	☒	A statement on whether measurements were taken from distinct samples or whether the same sample was measured repeatedly
☐	☒	The statistical test(s) used AND whether they are one- or two-sided *Only common tests should be described solely by name; describe more complex techniques in the Methods section.*
☐	☒	A description of all covariates tested
☐	☒	A description of any assumptions or corrections, such as tests of normality and adjustment for multiple comparisons
☐	☒	A full description of the statistical parameters including central tendency (e.g. means) or other basic estimates (e.g. regression coefficient) AND variation (e.g. standard deviation) or associated estimates of uncertainty (e.g. confidence intervals)
☐	☒	For null hypothesis testing, the test statistic (e.g. *F*, *t*, *r*) with confidence intervals, effect sizes, degrees of freedom and *P* value noted *Give P values as exact values whenever suitable.*
☒	☐	For Bayesian analysis, information on the choice of priors and Markov chain Monte Carlo settings
☒	☐	For hierarchical and complex designs, identification of the appropriate level for tests and full reporting of outcomes
☒	☐	Estimates of effect sizes (e.g. Cohen's *d*, Pearson's *r*), indicating how they were calculated

Our web collection on statistics for biologists contains articles on many of the points above.

Software and code

Policy information about availability of computer code

Data collection	no software was used for data collection
Data analysis	Alignment and preprocessing was performed using cellranger 3.1.0 (10X Genomics). Ambient RNA was removed using SoupX 1.2.2 and the data were processed using Seurat 3.1.4 in R 3.6.1. Cell-cell interaction analyses were performed using CellPhoneDB 2.1.2. Motif enrichment analyses were performed using Homer 4.10.0. Mixed model analysis was carried out in SPSS 26 (IBM), Mann-Whitney U tests and multiple/logistic regression analyses were run in Statistica (Tibco, version 13.3). Circos plots were generate using Circlize 0.4.10. Arboreto 0.1.5 and pySCENIC 0.10.0 were used with python 3.8.2 to infer transcription factor importance. Gene set enrichment analysis were performed using clusterProfiler 3.12.0. Bulk gene expression analyses of A549 cells were performed using limma 3.33.

For manuscripts utilizing custom algorithms or software that are central to the research but not yet described in published literature, software must be made available to editors/reviewers. We strongly encourage code deposition in a community repository (e.g. GitHub). See the Nature Research guidelines for submitting code & software for further information.

Data

Policy information about availability of data

All manuscripts must include a data availability statement. This statement should provide the following information, where applicable:

- Accession codes, unique identifiers, or web links for publicly available datasets
- A list of figures that have associated raw data
- A description of any restrictions on data availability

Due to potential risk of de-identification of pseudonymized RNA sequencing data the raw data will be available under controlled access in the EGA repository, [EGAS00001004772]. Count and metadata tables (patient-ID, sex, age, cell type, QC metrics per cell) can be found at FigShare: https://doi.org/10.6084/m9.figshare.13200278. In addition, these data can be visualized and analyzed in the Magellan COVID-19 data explorer at https://digital.bihealth.org. Beside newly generated and unpublished single cell transcriptome data of 31 patients, we also re-analyzed single cell transcriptome data of 17 previously published patients [EGAD00001006339]20, focusing on and addressing different biomedical questions. The human hg19 reference genome (version 3.1.0) or the SARS-CoV-2 genome

(Refseq-ID: NC_045512) used in this study can be found at https://cf.10xgenomics.com/supp/cell-exp/refdata-cellranger-hg19-3.0.0.tar.gz or https://www.ncbi.nlm.nih.gov/nuccore/1798174254, respectively.

Field-specific reporting

Please select the one below that is the best fit for your research. If you are not sure, read the appropriate sections before making your selection.

☒ Life sciences ☐ Behavioural & social sciences ☐ Ecological, evolutionary & environmental sciences

For a reference copy of the document with all sections, see nature.com/documents/nr-reporting-summary-flat.pdf

Life sciences study design

All studies must disclose on these points even when the disclosure is negative.

Sample size

No sample size calculation was performed. Sample size was determined according to maximal availability.

PaCOVID-19 cohort
Between March–May 2020, all COVID-19 patients that were hospitalized in Charité – Universitätsmedizin Berlin and willing to participate in the Pa-COVID-19 study were included in this study (in total 162 patients) . In the here presented study, we excluded patients that did not have their positive COVID-19 test at the Charité (n=12) and those with missing information on ACEi/ARB treatment (n=6). For the remaining 144 COVID-19 patients, we assessed differences in COVID-19 severity related to pre-existing cardiovascular diseases (CVD+), such as hypertension (HT+) or HT and an additional cardiac disease (coronary artery disease and/or heart failure, HT+/CVD+) in the different treatment groups (ACEi +, ARB+, ACEi-/ARB-) compared to patients without CVD (HT-/CVD-).

Single-cell RNA-seq cohort
We recruited all COVID-19 patients that were hospitalized in Charité or the University Hospital Leipzig from 11 March 2020 to 07 May 2020 that were willing to participate in this study. Controls were individuals hospitalized without having a SARS-CoV-2 infection and were tested negative for SARS-CoV-2 without common cold symptoms. All participants signed the informed consent. In total, we performed single cell RNA sequencing of 32 COVID-19 patients and 16 controls. Of the COVID-19 patients, 24 patients were classified as having severe, and nine as having critical disease according to the World Health Organization (WHO) guidelines. Baseline CVD were prevalent in 25 of the COVID-19 patients. They either suffered from HT only (n=16, 64%), CVD with HT (n=7, 28%), or CVD with heart failure and HT (n=2, 8%). Patients with HT only were classified as HT+, while all patients suffering from HT and CVD (and possibly additionally heart failure) were classified as HT+/CVD+. Concomitant treatment of HT+/CVD± included treatment with either ACEi (n=10) or ARB (n=15). Seven of the COVID-19 patients had no known CVD (21.2%). Note that patient BIH-SCV2-14 was included in all analysis regarding ACEi/ARB treatment but not in the CVD analysis (this patient suffered from HT and heart failure). Of the symptom-free SARS-CoV-2-negative patients, six had HT only (37.5%), and four had additional CVD (25%). Six of these patients received ACEi (37.5%) and four were treated with ARB (25%). The remaining six patients had no known CVD and therefore, were neither treated with ACEi nor ARB (37.5%).

Data exclusions

PaCOVID-19 cohort
Between March–May 2020, 162 COVID-19-positive patients were recruited at Charité – Universitätsmedizin Berlin in the Pa-COVID-19 study. In the here presented study, we excluded patients that did not have their positive COVID-19 test at the Charité (n=12) and those with missing information on ACEi/ARB treatment (n=6). For the remaining 144 COVID-19 patients, we assessed differences in COVID-19 severity related to pre-existing cardiovascular diseases (CVD+), such as hypertension (HT+/CVD-) or HT and an additional cardiac disease (coronary artery disease, CAD, and/or heart failure, HT+/CVD+) in the different treatment groups (ACEi+, ARB+, ACEi-/ARB-) compared to patients without HT-/CVD-.

Replication

Epidemiological replication/validation: In this study, we included all COVID-19 patients hospitalized at two university hospitals in Germany between 11 March 2020 to 07 May 2020, who were willing to participate in this study and signed the informed consent. For replication purposes an additional validation cohort would have been desirable. However, due to the limited number of hospitalized patients and restricted time-span of the COVID-19 pandemic in Germany, we were not able to recruit a sufficent number of patients as an independent replication cohort.

Technical replication: We performed single-cell RNA sequencing experiments. In general, no replicates are needed in single cell approaches. Note that we obtained high numbers of cells per patient and, in general, high quality sequencing libraries. Explanation: Sequencing several samples of the same patient at the same time point would have been prohibitively costly, reducing the number of biological replicates that would be feasible to include and thus ultimately the quality of the dataset. Furthermore, a cell could only be sequenced once, so adding a technical replicate would just add more cells for a patient. The per-sample cell numbers were already sufficient to estimate intra-patient heterogeneity, but in the context of the investigation of medical treatment, intra-patient heterogeneity is the more important measure.

Randomization

No randomization was performed as it was not applicable for this study.
We investigated two major patient groups; a "control group " and a "COVID-19 group".
Control group: Patients were tested negative for SARS-CoV-2 infection and showed no common cold symptoms (healthy controls).
COVID-19 group: All patients were tested positive for SARS-CoV-2 infection and were admitted to hospital due to their COVID-19-related symptoms. The disease severity was classified based on WHO guidelines and is described in the methods section. Note that all COVID-19 patients were admitted to the hospital, thus, we did not include mild cases or asymptomartic COVID-19 patients.

For regression analyses in the PaCOVID-19 cohort included further covariates as decribes in the method section of the manuscript.

Blinding

Blinding was not applicable for our study. Blinding would be performed in interventional studies to ensure that neither patient nor physician

Blinding	are aware of the grouping, i.e. the intervention received. It is not typically possible in observational studies such as this one, as no assignment to different treatment groups took place, with the patients receiving their usual treatment regimen.

Reporting for specific materials, systems and methods

We require information from authors about some types of materials, experimental systems and methods used in many studies. Here, indicate whether each material, system or method listed is relevant to your study. If you are not sure if a list item applies to your research, read the appropriate section before selecting a response.

Materials & experimental systems

n/a	Involved in the study
☒	☐ Antibodies
☐	☒ Eukaryotic cell lines
☒	☐ Palaeontology
☒	☐ Animals and other organisms
☐	☒ Human research participants
☒	☐ Clinical data

Methods

n/a	Involved in the study
☒	☐ ChIP-seq
☒	☐ Flow cytometry
☒	☐ MRI-based neuroimaging

Eukaryotic cell lines

Policy information about cell lines

Cell line source(s)	A549 cell line - lung carcinoma cells were obtained from the University Hospital Heidelberg. Original source: ATCC (CLL-185)
Authentication	A549 cells were authenticated by SNP profiling by a commercial service provider (Multiplexion, Immenstaad, Germany). Certificate available upon request.
Mycoplasma contamination	A549 cells were checked regularly for contamination with any of 14 different infectious agents, including mycoplasma spec. by a commercial service provider (Multiplexion, Immenstaad, Germany) and confirm that the A549 cells were tested negative for all contamination with any of thes agents. Certificate available upon request.
Commonly misidentified lines (See ICLAC register)	No commonly misidentified lines were used in this study

Human research participants

Policy information about studies involving human research participants

Population characteristics	Detailed descriptions of the cohorts used in this study are given in the methods section, figure 1c, extended data table 1 and 2. In the scRNAseq cohort, we investigated ten female and 23 male COVID-19 patients, age range 32 to 91 years. Based on the WHO guidelines, nine patients were classified as critical COVID-19 cases, while 24 patients were classified as severe COVID-19 cases. In addition, 16 SARS-CoV-2 negative controls were included as controls. Baseline cardiovascular disease (CVD) were prevalent in 25 of the COVID-19 patients: (HT) only (n=16), HT+CAD (n=7), or HT +CAD+heart failure (n=2); concomitant CVD-treatment with either ACEi (n=10) or ARB (n=15). Controls (SARS-CoV-2 negative): HT only (n=6), HT+CAD+ (n=4); ACEi (n=6) or ARB (n=4) treated; Additionally, we included six SARS-CoV-2 negative controls without CVD and thus without ACEi or ARB treatment. CVD = cardiovascular disease HT = hypertension CAD = coronary artery disease
Recruitment	1. All patients were informed about the study, willing to participate in this study and signed the respective informed consent 2. COVID-19 group: The patients needed to be clinically tested positive for SARS-CoV-2 infection and were either admitted to Charité or the University Hospital Leipzig. We chose the COVID-19 patients based on their pre-existing cardiovascular comorbidities with a focus on hypertension and coronary artery disease as well as ACEi or ARB treatment for the CVD. As all patients were hospitalized due to their COVID-19-related symptoms and no COVID-19 outpatients were recruited for this study, our study cohort is comprised of COVID-19 cases that showed rather strong infection-related symptoms. We were not able to investigate the cellular or transcriptional profiles of COVID-19 patients with only mild or no symptoms. 3. Control group: All controls were tested negative for SARS-CoV-2 and did not have any common cold symptoms. A subset of the control group was chosed based on their pre-existing cardiovascular comorbidities with a focus on hypertension and coronary artery disease as well as ACEi or ARB treatment for the CVD (to match the COVID-19 cohort). 4. We started sampling shortly after the pandemic reached Berlin/Leipzig with the first patients being hospitalized in Charité - Universitätsmedizin Berlin or University Hospital Leipzig, respectively. Patients were recruited from 11 March 2020 - 07 May 2020 6. All patients recruited in this study were >18 years old. We did not apply any restricitions regarding sex. 7. As all patients were recruited exclusively for this COVID-19 study and only after virus infection and admission to the hospital, we do not have any information about the transcriptional landscape of the patients before the infection. In addition, due to logistical reasons, we were not able to sample the patients after their recovery and hospital discharge.

8. Importantly, our cohort does not reflect the general patient distribution admitted to Charité or University Hospital Leipzig with regards to sex, age, or COVID-19 severity as the patients were randomly chosen based on their presence in the hospital and willingness to donate samples for this study.

Ethics oversight

This study was approved by the respective institutional ethics committee of either the Charité-Universitätsmedizin Berlin (EA2/066/20) or the University Hospital Leipzig (123/20-ek) and conducted in accordance with the Declaration of Helsinki.

Note that full information on the approval of the study protocol must also be provided in the manuscript.